BOEING

REV LTR

THE BOEING COMPANY
COMMERCIAL AIRPLANE DIVISION
P.O. BOX 707
RENTON, WASHINGTON 98055

CODE IDENT. NO. 81205

NUMBER D6-17094

TITLE: EXPERIMENTAL INVESTIGATION OF THE WALL PRESSURE FLUCTUATIONS IN SUBSONIC SEPARATED FLOWS

FOR LIMITATIONS IMPOSED ON THE USE OF THE INFORMATION CONTAINED IN THIS DOCUMENT AND ON THE DISTRIBUTION OF THIS DOCUMENT, SEE LIMITATIONS SHEET.

MODEL _____ CONTRACT _____

ISSUE NO. 18 ISSUED TO: DDC

"DISTRIBUTION OF THIS DOCUMENT IS UNLIMITED: IT MAY BE RELEASED TO THE GENERAL PUBLIC

PREPARED BY _____
A. M. Mohsen

SUPERVISED BY _____
G. E. Dowie

APPROVED BY _____ 1/30/67
G. B. Lange

APPROVED BY _____ 1/31/67 (DATE)
F. S. Holman

AD 4872 D

6-7000

THE BOEING COMPANY

NUMBER D6-17094
REV LTR

ACTIVE SHEET RECORD

SHEET NUMBER	REV LTR	ADDED SHEETS				SHEET NUMBER	REV LTR	ADDED SHEETS			
		SHEET NUMBER	REV LTR	SHEET NUMBER	REV LTR			SHEET NUMBER	REV LTR	SHEET NUMBER	REV LTR
TITLE						27					
A						28					
B						29					
C						30					
1						31					
2						32					
3						33					
4						34					
5						35					
6						36					
7						37					
8						38					
9						39					
10						40					
11						41					
12						42					
13						43					
14						44					
15						45					
16						46					
17						47					
18						48					
19						49					
20						50					
21						51					
22						52					
23						53					
24						54					
25						55					
26						56					

*SHEET A

THE BOEING COMPANY

NUMBER D6-17094

REVISIONS

LTR	DESCRIPTION	DATE	APPROVAL

ACKNOWLEDGMENTS

The author would like to express his appreciation to Mr. J. B. Large who initiated the research that evolved into the present report. The author is indebted to his thesis advisor, Professor A. F. Emery of the Department of Mechanical Engineering, University of Washington, for continued advice and cooperation.

The author also wishes to thank the staff of the Acoustics Laboratory and the Boundary Layer Facility for their assistance in the design of apparatus and in conducting the experiments.

TABLE OF CONTENTS

	Page
LIST OF FIGURES	2
NOMENCLATURE	4
REFERENCES	5
SUMMARY	6
1. Introduction	7
2. Results and Discussion	8
2.1 Velocity Profiles	8
2.2 Static Pressure Distribution	11
2.3 Wall Pressure Fluctuations	12
3. Conclusions	15
FIGURES	16
APPENDIX	48
FIGURES FOR APPENDIX	50

LIST OF FIGURES

Figure	Description	Page
1	Schematic Diagram of Regions of Separated Flow	16
2	Velocity Profiles of Oncoming Flow	17
3	Mean Velocity Profiles for 1 Inch Backward-Facing Step	18
4	Lampblack Trace Showing Flow Pattern on Floor of Test Section Behind 0.5 Inch Backward-Facing Step	19
5	Lampblack Trace Showing Flow Pattern on Floor of Test Section Behind 1.0 Inch Backward-Facing Step	20
6	Lampblack Trace Showing Flow Pattern on Floor of Test Section Behind 1.5 Inch Backward-Facing Step	21
7	Mean Velocity Profiles on Top of 1 Inch Forward-Facing Step	22
8	Lampblack Trace Showing Flow Pattern for 1.0 Inch Forward Facing Step	23
9	Mean Velocity Profiles and Turbulence Intensities for 1/2 Inch Fence	24
10	Lampblack Trace Showing Flow Pattern on Floor of Test Section Behind 0.5 Inch Fence	25
11	Lampblack Trace Showing Flow Pattern on Floor of Test Section Behind 1.0 Inch Fence	26
12	Summary Plot of the Pressure Coefficient for Forward-Facing Steps 0.5 and 1.0 Inches High, Backward-Facing Steps 0.5, 1.0, and 1.5 Inches High, and Fences 0.5 and 1.0 Inch High for Flow Speeds 170, 280, and 370 Ft/Sec	27
13	Pressure Coefficient for Backward-Facing Steps at 170 Ft/Sec	28
14	Pressure Coefficient for Backward-Facing Steps at 280 Ft/Sec	29
15	Pressure Coefficient for Backward-Facing Steps at 370 Ft/Sec	30
16	Pressure Coefficient for Forward-Facing Steps at 170 Ft/Sec	31
17	Pressure Coefficient for Forward-Facing Steps at 280 Ft/Sec	32
18	Pressure Coefficient for Forward-Facing Steps at 370 Ft/Sec	33
19	Pressure Coefficient for Half- and One-Inch Fences at 170 Ft/Sec	34
20	Pressure Coefficient for Half- and One-Inch Fences at 280 Ft/Sec	35

Figure	Description	Page
21	Pressure Coefficient for Half- and One-Inch Fences at 370 Ft/Sec	36
22	Summary Plot of Wall Pressure Fluctuations for Forward-Facing Steps 0.5 and 1.0 Inch High, Backward-Facing Steps 0.5, 1.0, and 1.5 Inghes High, and Fence 0.5 Inch High for Flow Speeds 170, 280, and 370 Ft/Sec	37
23	Fluctuating Pressure Distribution for Backward-Facing Steps at 170 Ft/Sec	38
24	Fluctuating Pressure Distribution for Backward-Facing Steps at 280 Ft/Sec	39
25	Fluctuating Pressure Distribution for Backward-Facing Steps at 370 Ft/Sec	40
26	Power Spectra for Half-Inch Backward-Facing Step at 370 Ft/Sec	41
27	Fluctuating Pressure Distribution for Forward-Facing Steps at 170 Ft/Sec	42
28	Fluctuating Pressure Distribution for Forward-Facing Steps at 280 Ft/Sec	43
29	Fluctuating Pressure Distribution for Forward-Facing Steps at 370 Ft/Sec	44
30	Power Spectra for Half-Inch Forward-Facing Step at 370 Ft/Sec	45
31	Fluctuating Pressure Distribution for Half-Inch Fence	46
32	Power Spectra for Half-Inch Fence at 370 Ft/Sec	47
A.1	Diagram of Boeing Subsonic Boundary Layer Facility	50
A.2	Longitudinal Cross-Section of Test Section	51
A.3	Test Section for Study of Separated Flow	52
A.4	Motor-Driven Traverse Mechanism	53
A.5	Diagram of Instrumentation for Recording Wall Pressure Fluctuations	54
A.6	Various Measuring Probes	55
A.7	Manually Operated Traverse Mechanism with Zero-Velocity Probe Adapted	56

NOMENCLATURE

C_p	= Pressure coefficient
f	= Frequency, cps
h	= Height of configuration, in.
L	= Characteristic length, in.
p_o	= Reference static pressure, lb/ft^2
p_x	= Local static pressure, lb/ft^2
$\sqrt{\overline{p^2}}$	= Root mean squared (rms) fluctuating pressure, lb/ft^2
p^2 (f)	= Power spectral density of fluctuating pressure, $(lb/ft^2)^2/cps$
q	= Dynamic pressure, lb/ft^2
u	= Local longitudinal velocity, ft/sec.
U_∞	= Velocity at duct centerline, ft/sec.
$\sqrt{\overline{u'^2}}/U$	= Turbulence intensity in direction of flow
$(\overline{u'v'})$	= Reynolds stress, $(ft/sec)^2$
x	= Longitudinal distance in direction of flow, in.
y	= Lateral distance normal to flow, in.
δ	= Boundary layer thickness, in.
ρ	= Air density, $slug/ft^3$
θ	= Momentum thickness, in.

REFERENCES

1. H. W. Liepmann, "The Interaction Between Boundary Layer and Shock Waves in Transonic Flow," Journal of Aeronautical Sciences, Vol. 13, No. 12, December 1946, pp. 623-637

2. Dean R. Chapman and Edward W. Perkins, Experimental Investigation of the Effects of Viscosity on the Drag of Bodies of Revolution at a Mach Number of 1.5, NACA RM A7A31a, 1947

3. Dean R. Chapman, Donald M. Kuenn, and Howard K. Larson, Investigation of Separated Flows in Supersonic and Subsonic Streams with Emphasis on the Effect of Transition, NACA Rep. 1356

4. H. H. Korst, R. H. Page, and M. E. Childs, A Theory for Base Pressure in Transonic and Supersonic Flow, TN 392-2, University of Illinois, Engineering Experimental Station, Mechanical Engineering Department, March 1955

5. A. L. Kistler, "Fluctuating Wall Pressure Under a Separated Supersonic Flow," Journal of the Acoustical Society of America, Vol. 36, No. 3, March 1964, pp. 543-550

6. W. V. Speaker and C. M. Ailman, Spectra and Space-Time Correlations of the Fluctuating Pressures at a Wall Beneath a Supersonic Turbulent Boundary Layer Perturbed by Steps and Shock Waves, NASA CR-486

7. R. A. Seban, "Heat Transfer to the Turbulent Separated Flow of Air Downstream of a Step in the Surface of a Plate," Trans. ASME, Journal of Heat Transfer, May 1964, pp. 259-264

8. R. A. Seban, A. Emery, and A. Levy, "Heat Transfer to Separated and Reattached Subsonic Turbulent Flows Obtained Downstream of a Surface Step," Journal of Aeronautical Sciences, Vol. 26, No. 12, December 1959, pp. 809-814

9. I. Tani, Experimental Investigation of Flow Separation Over a Step, Boundary Layer Research, Frieburg Symposium, Springer, Germany, 1957

10. M. Arie and H. Rouse, "Experiments on Two-Dimensional Flow Over a Normal Wall," Journal of Fluid Mechanics, Vol. 1, July 1956

11. J. D. Revell and R. E. Gleason, Turbulent Wall Pressure Fluctuations Under Separated Supersonic and Hypersonic Flows, AFFDL-TR-65-77

SUMMARY

Experimental measurements of static pressures, fluctuating wall pressures, and mean velocity profiles are presented for subsonic turbulent separated flows. Separation was induced by three types of geometrical configurations: Backward-facing steps 1/2, 1, and 1-1/2 inches high; forward-facing steps 1/2 and 1 inch high; and fences 1/2 and 1 inch high. Measurements were made for free stream velocities of 170, 280, and 370 ft/sec.

It was found that the base pressure was essentially Reynolds number independent. The separation length was independent of speed and proportional to the height of the configuration causing flow separation.

The wall pressure fluctuations associated with the separated flows were of higher magnitudes than those caused by attached turbulent boundary layers and reached maximum values near reattachment.

EXPERIMENTAL INVESTIGATION OF THE WALL PRESSURE FLUCTUATIONS IN SUBSONIC SEPARATED FLOWS

1. INTRODUCTION

Flow separation occurs on the surfaces of airplanes for a variety of reasons: a sudden change in contour, as in the vicinity of the cabin windshield, a deflected control surface, or a discontinuity in the skin, as in the case of window cut-outs. The fluctuating forces associated with separated flows are known to be of higher magnitudes than those which result from attached turbulent boundary layers. These fluctuating forces cause structural vibrations which radiate sound of unacceptable levels in cabin interiors and may cause localized sonic fatigue.

Future structural design practice will require specification of the forcing field produced by separated flows. This will involve the determination of the magnitudes of the static and fluctuating forces over the length of separation region as well as the frequency spectral distribution of the energy in the forcing field.

A large number of experimental and theoretical investigations have been undertaken to study the structure of separated flows. Most of these investigations have emphasized phenomena such as the effects of transition on separation (References 1 and 2), the flow conditions near reattachment (Reference 3), and the base pressure problem (Reference 4). Although these studies have helped in understanding the dynamics of separated flows, the problem of the fluctuating forces associated with them is yet to be adequately defined for structural design purposes.

In the supersonic regime, Kistler (Reference 5) has measured the wall pressure fluctuations under a separated flow upstream of a forward-facing step. Speaker and Ailman (Reference 6) have reported on the fluctuating pressures resulting from separation for backward-facing and forward-facing steps. However, no measurements of the fluctuating pressures under subsonic separated flows have been reported. In view of this lack of information, and because of the above mentioned necessity for describing the forcing field on airplane components subjected to subsonic separated flows, the following experimental study was carried out.

Three geometrical configurations were selected as being most representative of those producing separated flows on airplanes: backward-facing steps, forward-facing steps, and fences. The heights of the geometries of this study were selected smaller

than the thickness of the incoming boundary layer for modeling of practical cases. The objective of this investigation was to measure for these configurations (1) position and extent of separation, (2) magnitudes of static and fluctuating forces, and (3) frequency spectra of the fluctuating forcing field. The boundary layer of the oncoming attached flow was turbulent and had an effective thickness of 2 inches. All measurements were taken at the Boeing Subsonic Boundary Layer Facility.

2. RESULTS AND DISCUSSION

2.1 Velocity Profiles

A description of the apparatus and measuring procedures used in these experiments is given in the Appendix.

Separate traverses of the total and static pressures were made in the oncoming attached flow and streamwise in the regions of separation and reattachment. All traverses were confined to the vertical plane containing the centerline of the test section. A schematic diagram of the various regions of the flow is shown in Figure 1. By applying Bernoulli's equation in the form

$$\frac{u}{U_\infty} = \left\{ \frac{P_t - P_s}{\frac{1}{2} \rho U_\infty} \right\}^{1/2}$$

to the pressure measurements, non-dimensional velocity profiles for the various configurations and speeds of this experiment were obtained. Because it was found that the profiles, for any one configuration, did not change significantly with height or speed, only a typical profile history per configuration is presented. In these profiles, shown in Figures 3, 7, and 9, the location of the $u = 0$ line was determined experimentally using the probe and technique described in the Appendix. The line joining the inflection points in the velocity profiles approximately locates, in the free shear layer, the region of maximum turbulent stress. It is to be noted that the magnitudes of the velocities in the reversed flow region are only approximate because of the skewness of the flow in this region with respect to the measuring probes.

A summary of the separation lengths for three different configurations is given in the following table.

Configuration	Separation Length x/h
Backward-facing step	5
Forward-facing step	2
Fence	11

2.1.1 Oncoming Flow

Figure 2 shows the velocity profiles of the oncoming flow for air speeds of 170, 280, and 370 ft/sec. For all speeds, the effective boundary layer was turbulent and was 2 inches thick. The vertical distance, y, was normalized by the boundary layer momentum thickness, θ, and the local longitudinal component of the velocity, u, by the centerline velocity, U_∞, measured upstream of the steps and fences. The profiles obeyed the 7th power law and were identical in shape to flat plate turbulent boundary layers at zero incidence.

2.1.2 Backward-Facing Step

Shown in Figure 3 is a spatial distribution of the velocity profiles for a 1-inch backward-facing step at an air speed of 370 ft/sec. It is seen that, in the region of flow reversal, the magnitudes of the velocities are rather small compared to the free stream velocity and the ratio u/U_∞ does not exceed one fourth. This is in close agreement with the measurements of Reference 7 in which the ratio u/U_∞ in the region of flow reversal behind a 1-inch backward-facing step at an air speed of 150 ft/sec is shown to be less than 0.2. The shape of the $u = 0$ line is indicative of expansion of the flow as it passes over the step. The line fitted through the inflection points of the velocity profiles serves to approximately locate the line of maximum turbulent shear stress $(\overline{u'v'})_{max}$ as will be discussed in a later section. The velocity profile near reattachment is typical in shape to that of an attached boundary layer advancing in an adverse pressure gradient. This can be explained by the pressure rise which accompanies reattachment. The flow pattern on the floor of the test section was visually observed by means of the lampolack traces shown in Figures 4, 5, and 6 for 0.5, 1.0, and 1.5 inch high backward-facing steps, respectively. These figures show that the flow is three-dimensional except for the narrow region containing the centerline of the test section. There exists a line of small vortices along the transverse edge of the step with a large vortex occurring at each end of the line. For this configuration, reattachment is shown to occur between 4 and 5 step heights and was found to be independent of speed. This length to reattachment is in good agreement with that reported by Reference 8 in which reattachment downstream of backward-facing steps, at air speeds and

step heights similar to those of the present experiment, was found to be five step heights.

2.1.3 Forward-facing Step

Figure 7 shows the distribution of longitudinal velocity components for a forward-facing step at an air speed of 370 ft/sec. From the shape of the $u = 0$ line, it is seen that the flow overshoots as it passes the face of the step resulting in a region of flow reversal on top of the step. The maximum height of the reversed flow region is small in comparison with the step height and does not exceed two-tenths of the step height. As in the case of the backward-facing step, the shape of the velocity profile near reattachment indicates the pressure rise which occurs at reattachment. The length of the separation region, as observed by means of lampblack traces shown in Figure 8, was found to be between 2 and 2.5 step heights and increased very slightly with air speed.

2.1.4 Fence

Mean velocity profiles and turbulence intensities for a 1/2-inch fence at an air speed of 280 ft/sec are shown in Figure 9. The shape of the $u = 0$ line indicates that the flow overshoots as it passes over the fence to a height slightly larger than that of the fence. This overshoot results, behind the fence, in a region of flow reversal which is longer for a fence than for a backward-facing step of the same height. The separation length for 1/2- and 1-inch fences was visually observed, see Figures 10 and 11, to be between 11 and 12 fence heights, and was found to be independent of speed. Figures 10 and 11 also show that the flow is three-dimensional and that a line of vortices exists behind the fence. As in the cases of backward-facing and forward-facing steps, the velocity profiles near reattachment display the shape imposed on a profile by a positive pressure gradient.

The turbulent intensity measurements, presented in figure 9, show that the line joining the maxima of the turbulent shear stress, $(\overline{u'v'})_{max}$, and the line fitted through the inflection points in the velocity profiles have the same ordinates. Under the assumption that a comparable relationship holds for backward- and forward-facing steps, it was possible to locate for these configurations the line $(\overline{u'v'})_{max}$, as shown in Figures 3 and 7. The magnitudes and shapes of the turbulence intensities, $\sqrt{\overline{u'^2}}/U_\infty$, downstream of the fence are in good agreement with those reported in Reference 9 with peak intensities of 25% occurring in the free shear layer.

2.2 Static Pressure Distribution

The static pressure distribution along the centerline of the base of the test section was recorded for the speeds and configurations tested. The results of these measurements are shown in Figures 13 to 21. In these results, the distance, x, is normalized by the height, h, of the geometry causing flow separation. The pressure coefficient, C_p, is given by

$$C_p = \frac{p_\infty - p_0}{\frac{1}{2} \rho U_\infty^2}$$

where p_0 is a reference pressure measured upstream 1 inch from the backward-facing steps and 14 inches from the forward-facing steps and fences. A summary plot of the results of this section is shown in Figure 12.

2.2.1 Backward-Facing Step

Shown in Figures 13, 14, and 15 are the pressure distributions downstream of backward-facing steps 0.5, 1.0, and 1.5 inch high for air speeds of 170, 280, and 370 ft/sec. As seen from these figures, immediately behind the steps, the pressure coefficient is negative and becomes slightly more negative with increase in distance to about 3 step heights. Between $x/h = 3$ and $x/h = 5$, the pressure rises very rapidly and becomes positive. With further increase in distance the pressure reaches a maximum positive value and then drops gradually and approaches ambient pressure.

It is interesting to note that the base pressure is essentially insensitive to changes in step height or speed, which is in agreement with observations made in Reference 4. The rapid rise in pressure is indicative of flow reattachment which, for backward-facing steps, was visually observed to occur between 4 and 5 step heights (see Figures 4, 5, and 6).

2.2.2 Forward-Facing Step

In the case of the forward-facing steps, shown in Figures 16, 17, and 18, the pressure begins to rise above ambient as the flow approaches the step face where the pressure reaches a maximum positive value. On top of the step, where the flow is separated, the pressure starts at a negative value at $x/h = 0$ and increases to ambient at 8 to 9 step heights. Flow reattachment occurs between 2 to 2.5 step heights but is not accompanied with a sudden rise in pressure. The pressure distribution upstream and downstream of the step is found to be independent of speed.

2.2.3 Fence

The pressure distribution downstream of fences 0.5 and 1.0 inch high at airspeeds 170, 280, and 370 ft/sec are presented in Figures 19, 20, and 21. The cavity length for the fences is twice as long and has a pressure coefficient 3 times as negative as the backward-facing steps. The region of rapid pressure rise is longer for the fences than that for the backward-facing steps, 8 fence heights versus 2 step heights. Reattachment for fences, as observed visually in Figures 10 and 11, occurs between 11 and 12 fence heights and is independent of speed.

2.3 Wall Pressure Fluctuations

Presented in this section are power spectral density measurements of wall pressure fluctuations along the centerline of the test section in regions of undisturbed, separated, and reattached flow. The root mean square of wall pressure fluctuations, $\sqrt{\overline{p'^2}}$, were computed from the relation

$$\sqrt{\overline{p'^2}} = \left\{ \int_{f_1}^{f_2} p^2(f)\, df \right\}^{1/2}$$

For this experiment, because of background noise from extraneous sources, below a frequency of 200 cps, the lower limit of the above integral, f_1, was taken at 200 cps. The upper limit, f_2, of the integral was determined by the dynamic range of the instrumentation. A summary plot of fluctuating pressures for the various geometries of this experiment is shown in Figure 22.

2.3.1 Backward-Facing Step

Shown in Figures 23, 24, and 25 are over-all r.m.s. values of wall fluctuating pressure levels normalized by the free stream dynamic pressure, q_∞, for three backward-facing steps 0.5, 1.0 and 1.5 inch high at air speeds of 170, 280, and 370 ft/sec. The distance, x, is normalized by the step height, h. These figures show that a short distance behind the step, $x/h = 1/2$, the fluctuating pressure levels are only slightly higher than those of the corresponding undisturbed flow upstream of the steps. The levels continue to increase with distance and reach maximum values between $x/h = 4$ and 5, which coincides with the region of flow reattachment for backward-facing steps.

In Reference 6, it was found, for a backward-facing step 0.74 inches high at Mach numbers of 1.4 and 3.5, that maximum fluctuating pressure levels occurred in the region of reattachment. Past reattachment, the fluctuating pressure levels decrease gradually with

increase in distance but do not reach the undisturbed flow levels within a distance x/h = 7.5, beyond which no measurements were taken.

From these results, it is seen that the ratio $\sqrt{\overline{p'^2}}/q_\infty$ is independent of step height and air speed.

Shown in Figure 26 are typical spectra of the pressure fluctuations in the regions of separation and reattachment behind a 0.5 inch backward-facing step. The spectra shows that immediately behind the step, at x/h = 0.5, most of the energy is contained in the low frequency end of the specturm. As the region of reattachment is approached, x/h = 3.0, the low frequency level of the spectrum increases slightly and more energy is added in the mid-frequency range. In the reattachment region, x/h = 4.5, it is important to note that the shape of the spectrum is essentially the same as that at x/h = 3.0 but is of higher level and is shifted to a higher frequency range. Past reattachment, x/h = 7.5, the level of the spectrum decreases and most of the energy is concentrated in the middle frequency range of the spectrum typical of the shape of attached turbulent flow spectra.

2.3.2 Forward-Facing Step

Shown in Figures 27, 28, and 29 are ratios of $\sqrt{\overline{p'^2}}/q_\infty$ plotted against x/h upstream and downstream of forward-facing steps 0.5 and 1.0 inch high for air speeds 170, 280, and 370 ft/sec. As seen from these results, the fluctuating pressure levels begin to increase above the undisturbed flow levels approximately 3 step heights upstream of the face of the step and continue to increase rapidly as the face of the step is approached. The levels reach maximum values on top of the step at x/h = 1.5 slightly before reattachment which, for a forward-facing step, occurs between x/h = 2 and 2.5.

These results, show that for each air speed the fluctuating pressure levels are independent of step height and air speed.

Typical spectra upstream and downstream of a forward-facing step are shown in Figure 30. From these spectra, it is seen that upstream of the step, at x/h = -3.0, most of the energy is contained in the low frequency end of the spectrum. On top of the step, in the separated flow region, at x/h = 1.5, more energy is added in the mid-frequency range and the spectrum is of much higher level and has a larger band-width than at x/h = -3.0.

Immediately behind reattachment, at x/h = 3.0, the low frequency energy begins to drop in magnitude and more energy is added in the mid-frequency range. At x/h = 3.75, the spectrum, although of higher level, is similar in shape to that of turbuelnt boundary layers with a large portion of the energy appearing in the mid-frequency range.

2.3.3 Fence

Over-all r.m.s. values of fluctuating pressure levels downstream of a 0.5-inch fence for air speeds 170, 280, and 370 ft/sec are presented in Figure 31.

The levels behind the fence x/h = 1.5, are higher than the undisturbed flow levels and continue to increase with increase in distance downstream of the fence and reach maximum values around x/h = 8.5 slightly before reattachment which, for fences, occurs between x/h = 11 and 12. The ratio $\sqrt{\overline{p^2}}/q_\infty$ increases slightly with increase in speed, but the increase is larger between 170 ft/sec and 280 ft/sec than between 280 ft/sec and 370 ft/sec.

Figure 32 shows the variation of shape and level of the spectra with increase in distance downstream of the fence. Unlike the spectra for backward-facing and forward-facing steps, the shape of the spectra for the fence are essentially the same with low frequency energy added with increase in distance, to the point of maximum fluctuating pressure level, then low frequency energy is subtracted resulting in a lower level. The rolling-off of the spectra is rather rapid and the spectra are contained in fairly narrow band-width.

2.3.4 Interpretation of Fluctuating Pressure Distribution

A possible explanation for the distribution of the wall pressure fluctuations under separated flows, and in particular for the occurrence of maximum fluctuating pressures near reattachment can be made from the flow model presented in Reference 4. In this model, the oncoming attached boundary layer, past the point of separation, becomes a free mixing shear layer. The thickness of this layer increases with distance to reattachment. The compression at reattachment thickens the boundary layer beyond its rate of growth as a free shear layer. Reference 11 shows that for attached flows

$$\sqrt{\overline{p^2}}/q_\infty \sim \left(\frac{\delta}{L}\right)^{3/2}$$

where L is a characteristic length. For attached turbulent flow, the fluctuating pressures are also proportional to the turbulent shear stress $(\overline{u'v'})$. References 9 and 10 show that the turbulent shear stress in the free shear layer increases with increase in distance from the point of separation. Reference 5 suggests that for separated flow, the pressure fluctuations are probably proportional to the shear in the free mixing layer.

From the above, it is therefore reasonable to assume that the monotonic increase of fluctuating pressure levels in the region of separation is due chiefly to the increase with distance of $(\overline{u'v'})_{max}$. In the reattachment region, added to the shear stress is the pronounced thickening of the boundary layer. These combined effects would account for the maximum levels of the wall pressure fluctuation near reattachment.

3. Conclusions

From the results of this experimental investigation, the following conclusions can be made. The base pressure, in the region of flow reversal, is essentially independent of increase in step height and air speed. The length of the separation region, however, is more dependent on the height of the configuration causing flow separation than on increase in speed.

The increase of the turbulent shear stress in the free shear layer with distance from the point of separation results from the interaction between the reversed flow and the main flow. This increase in shear stress could account for the monotonic increase in fluctuating pressure levels that were observed in the region of flow reversal. At reattachment, the occurrence of maximum fluctuating pressure could be the result of the combined effects of the shear stress and the thickening of the shear layer. However, for this to become conclusive, further experimental work is required to establish the relation between shear stress, shear layer thickness, and fluctuating pressure levels.

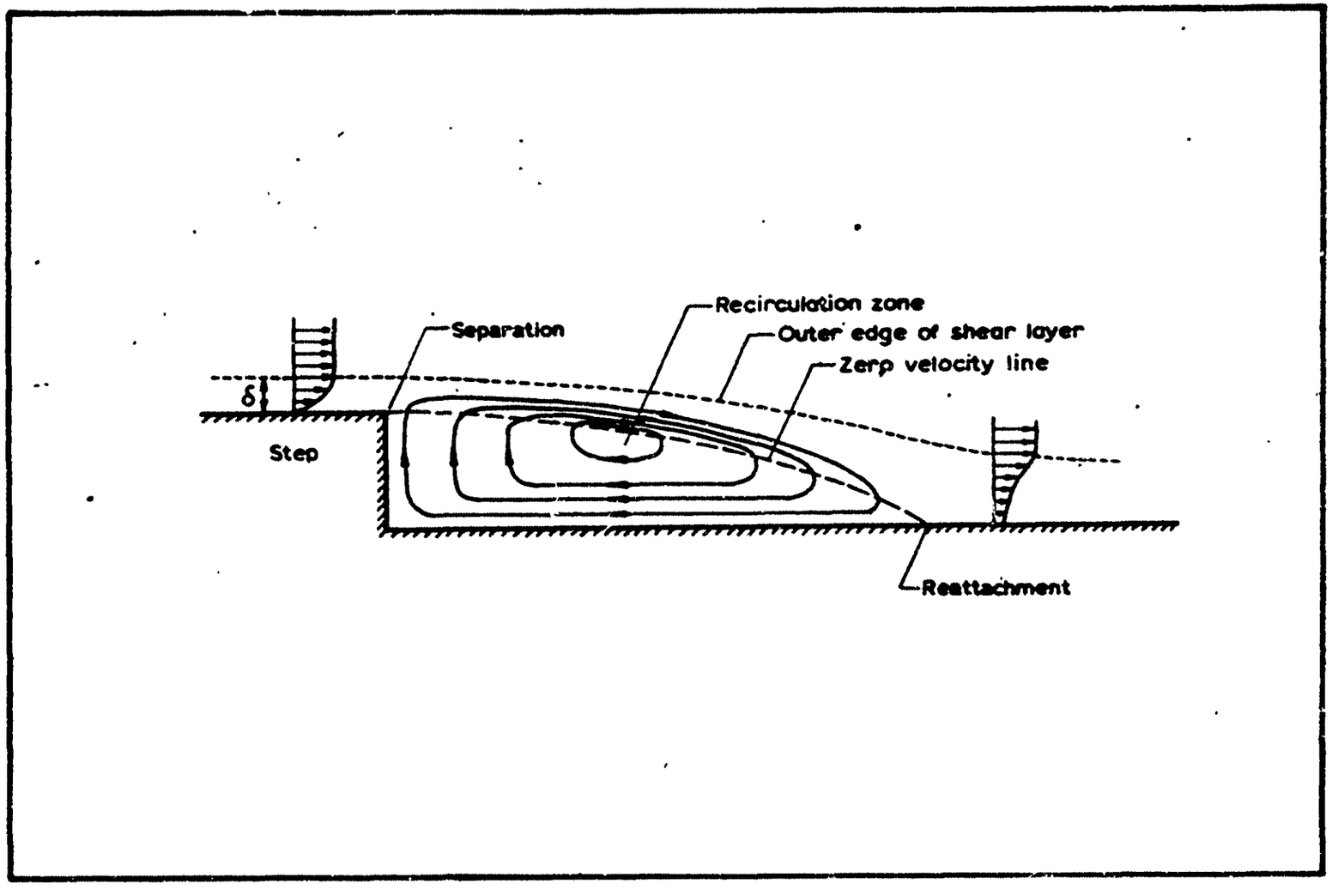

FIGURE 1. SCHEMATIC DIAGRAM OF REGIONS OF SEPARATED FLOW

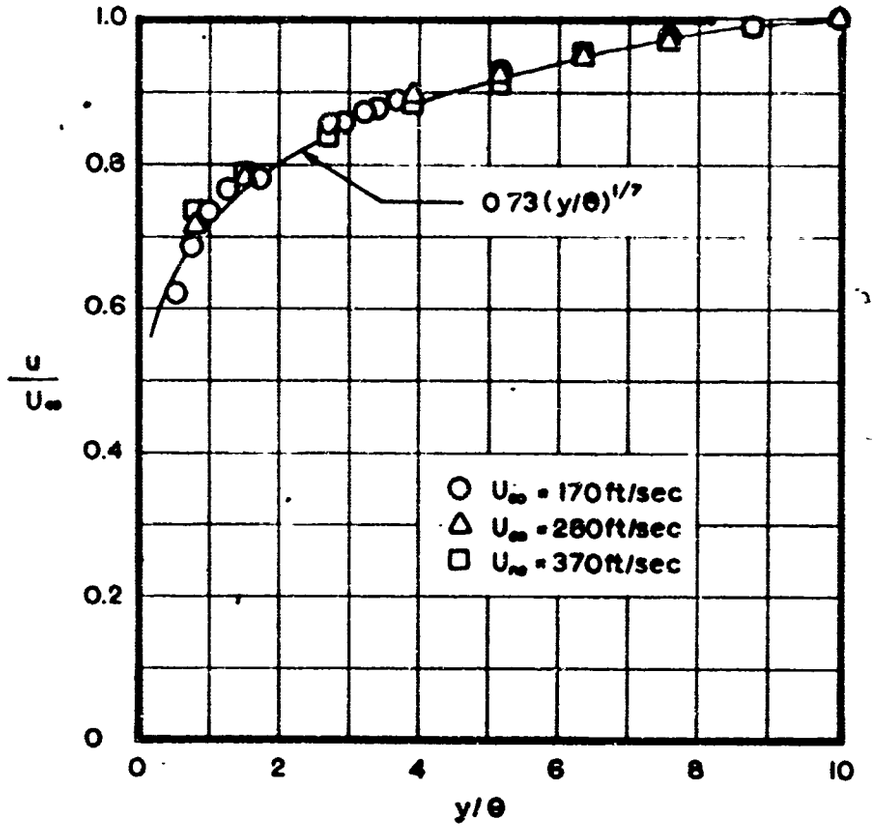

AD 1546 D

REV SYM

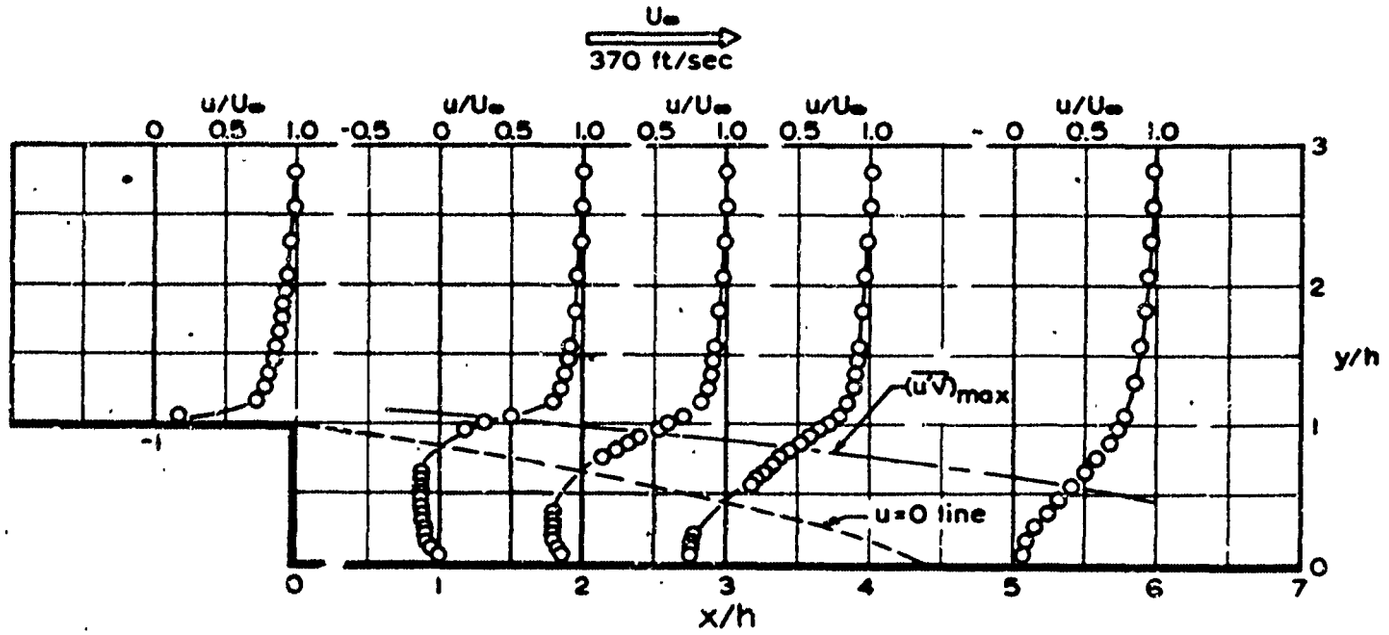

FIGURE 9. MEAN VELOCITY PROFILES FOR FLAT AFTERBODY

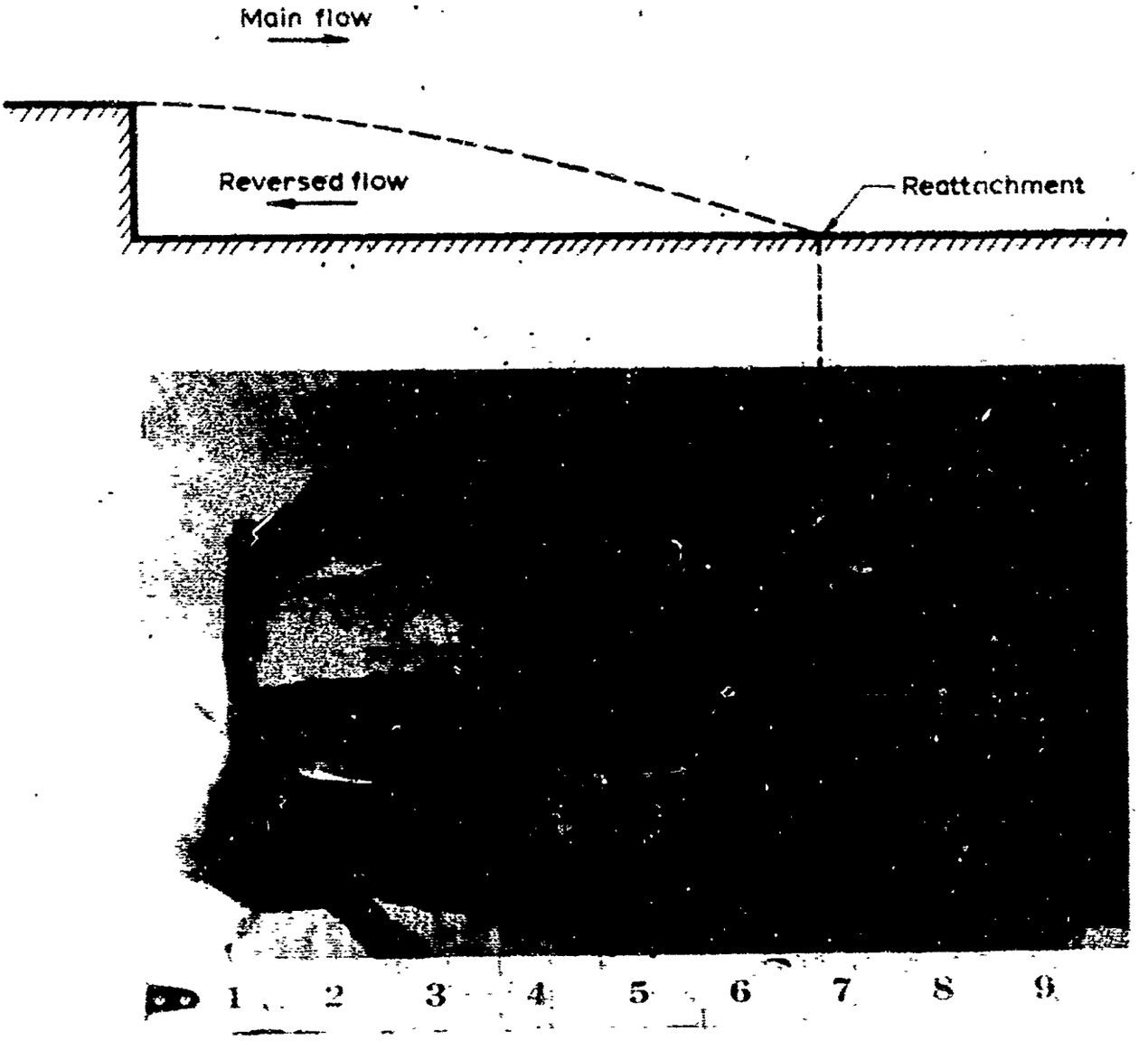

6. [illegible] FLOW PATTERN [illegible] 1.5 INCH BACKWARD-FACING [illegible]

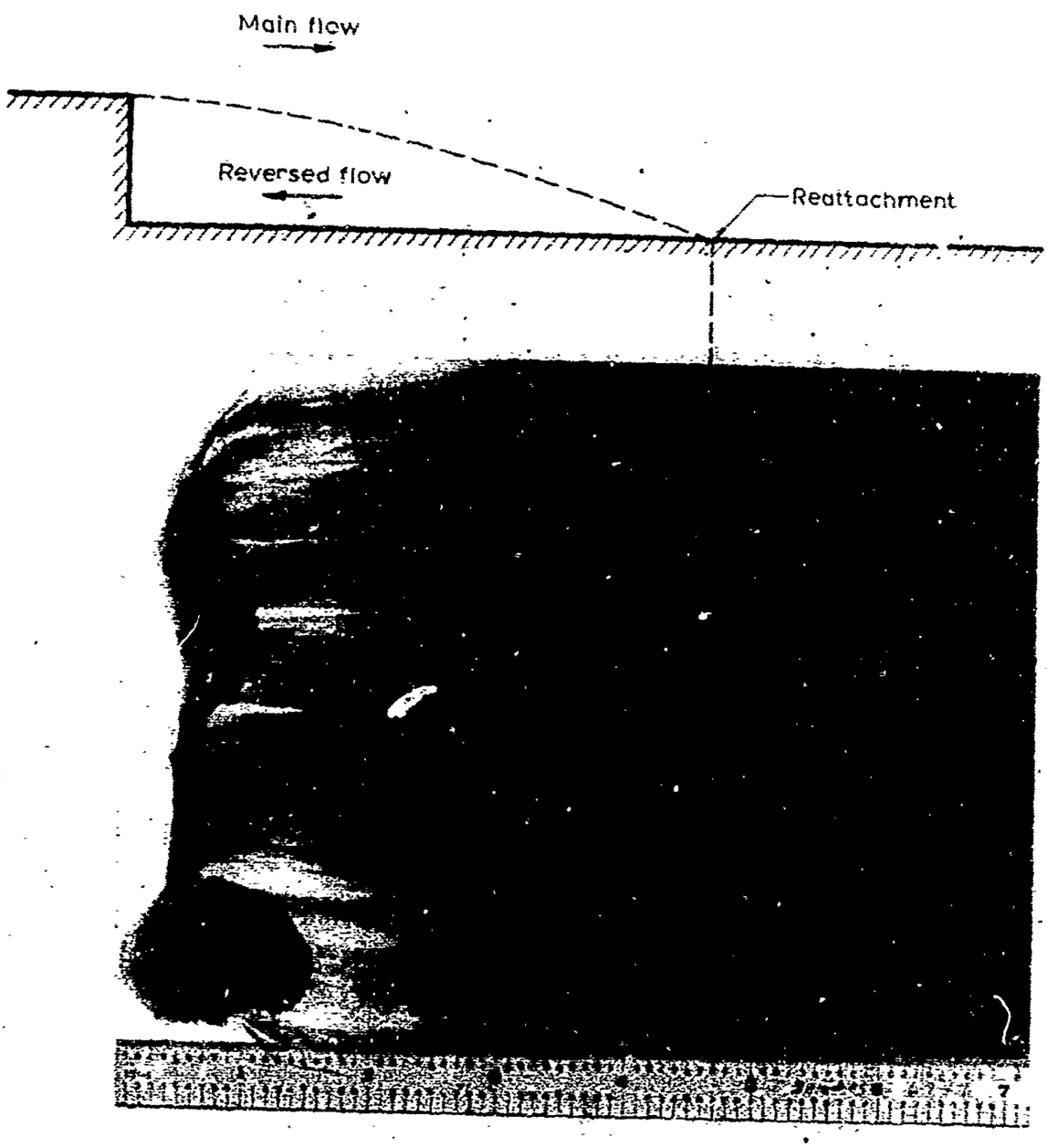

FIGURE 5. [illegible] FLOW PATTERN ON FLOOR [illegible] FLOW BEHIND 1.0 INCH BACKWARD-FACING STEP.

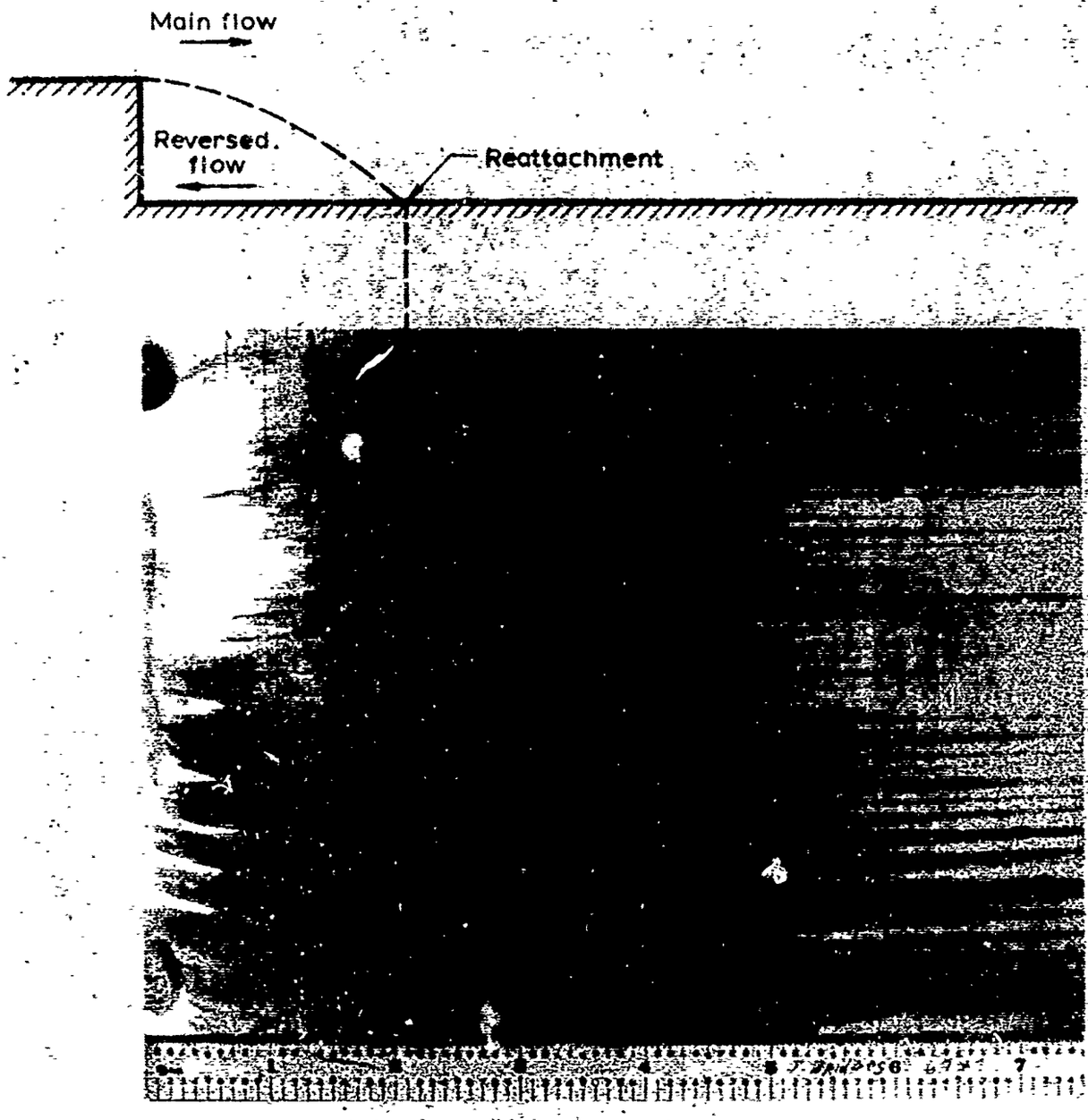

FIGURE 4. LAMPBLACK TRACE SHOWING FLOW PATTERN ON FLOOR OF TEST SECTION BEHIND 0.5 INCH BACKWARD-FACING STEP.

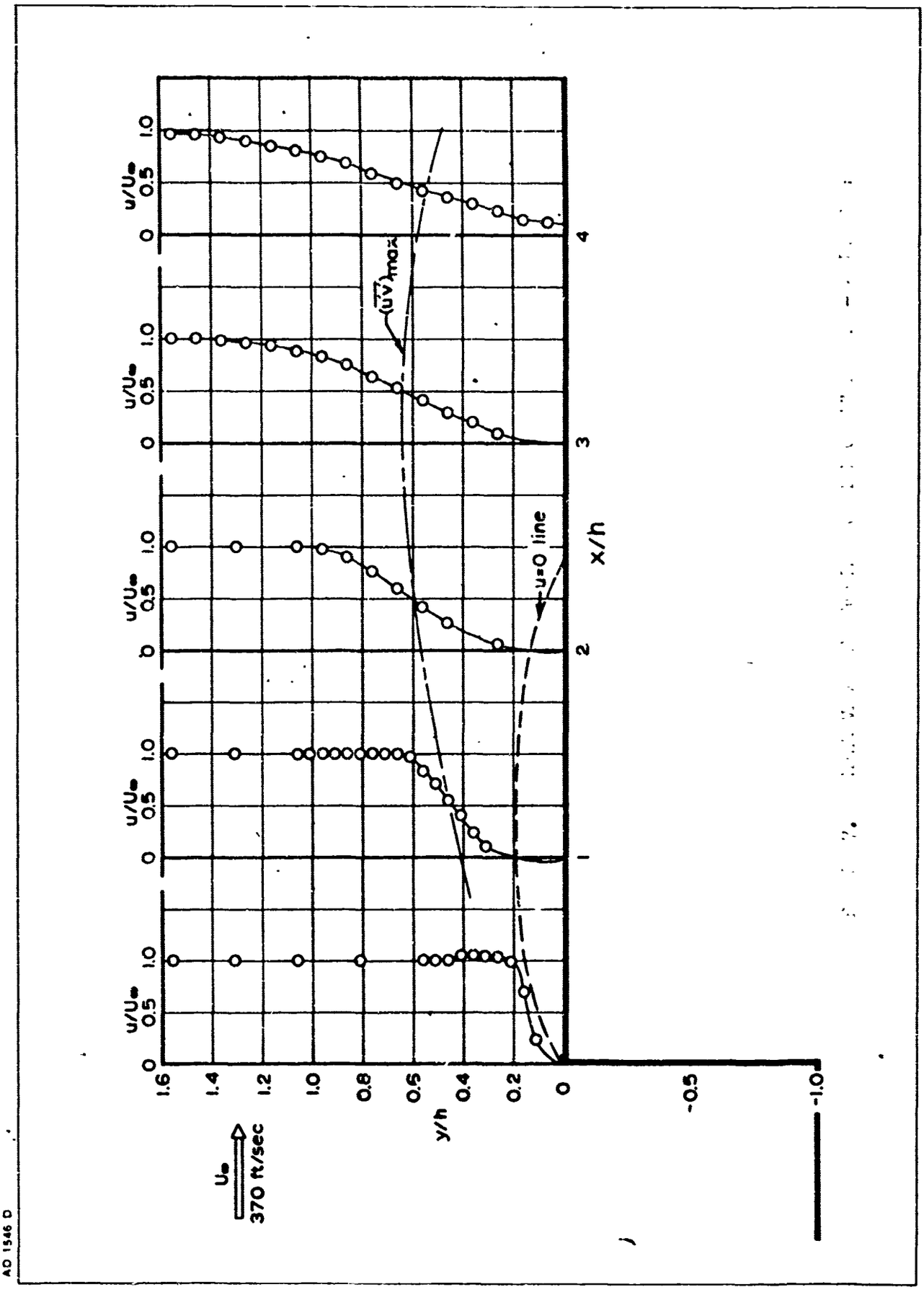

AD 1546 D

REV SYM

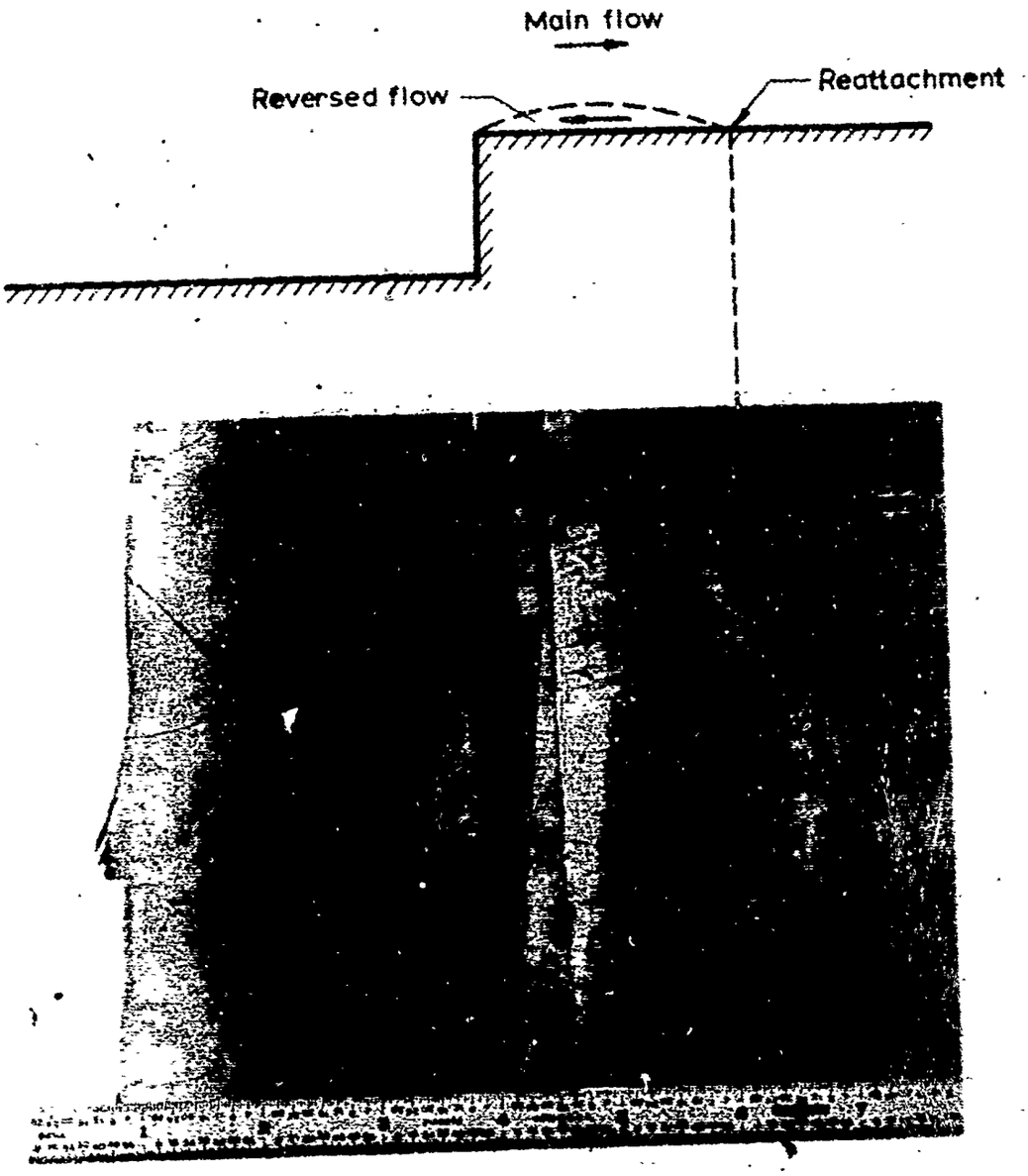

FIGURE 8. LAMINAR BLACK-TRACE SMOKING FLOW PATTERN FOR 1.0 INCH FORWARD-FACING STEP.

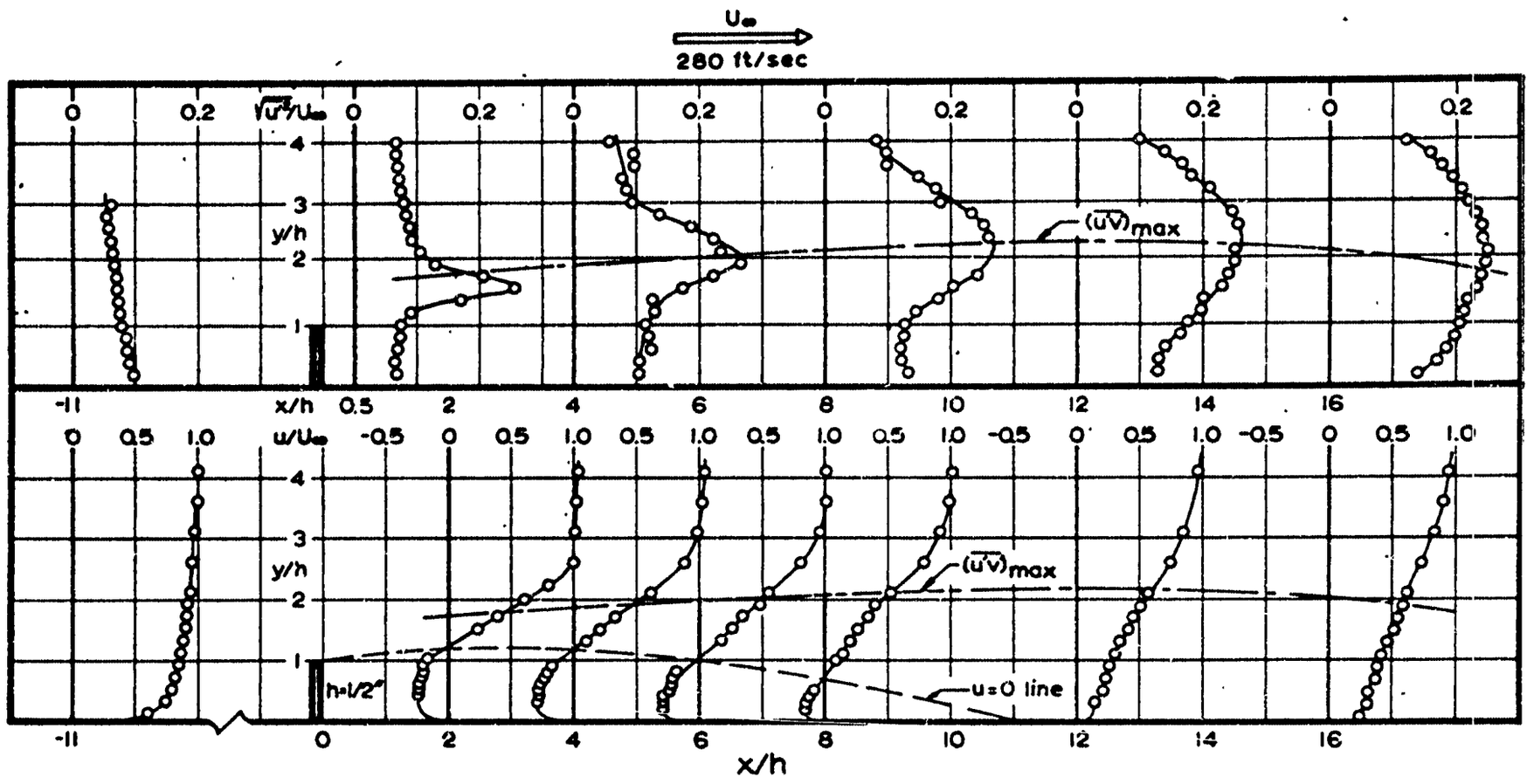

FIGURE 2. MEAN VELOCITY PROFILES IN TURBULENT BOUNDARY LAYER AT 1/2" FS

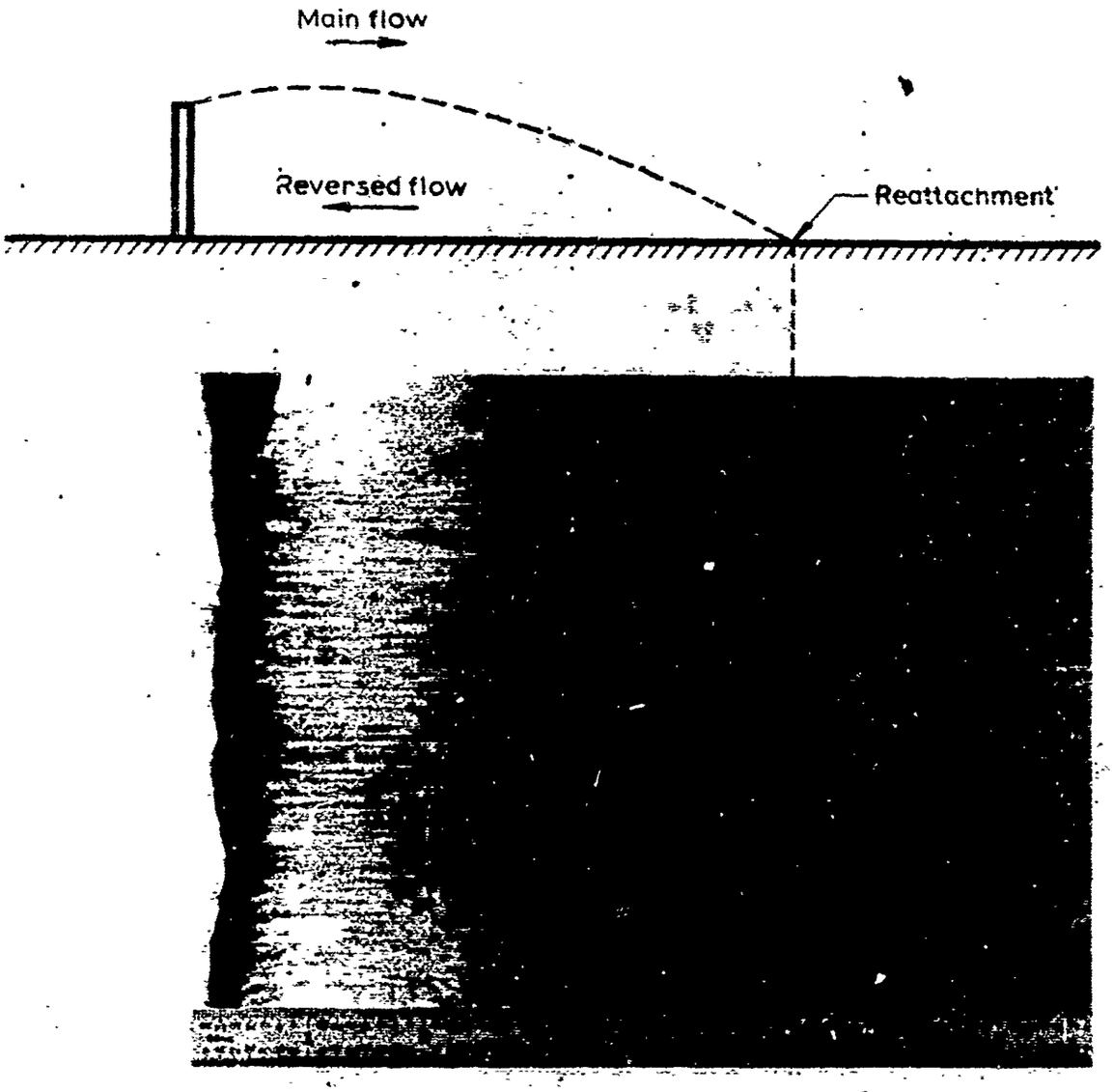

FIGURE 10. LAMPBLACK TRACE SHOWING FLOW PATTERN ON FLOOR OF TEST SECTION BEHIND 0.5 INCH FENCE.

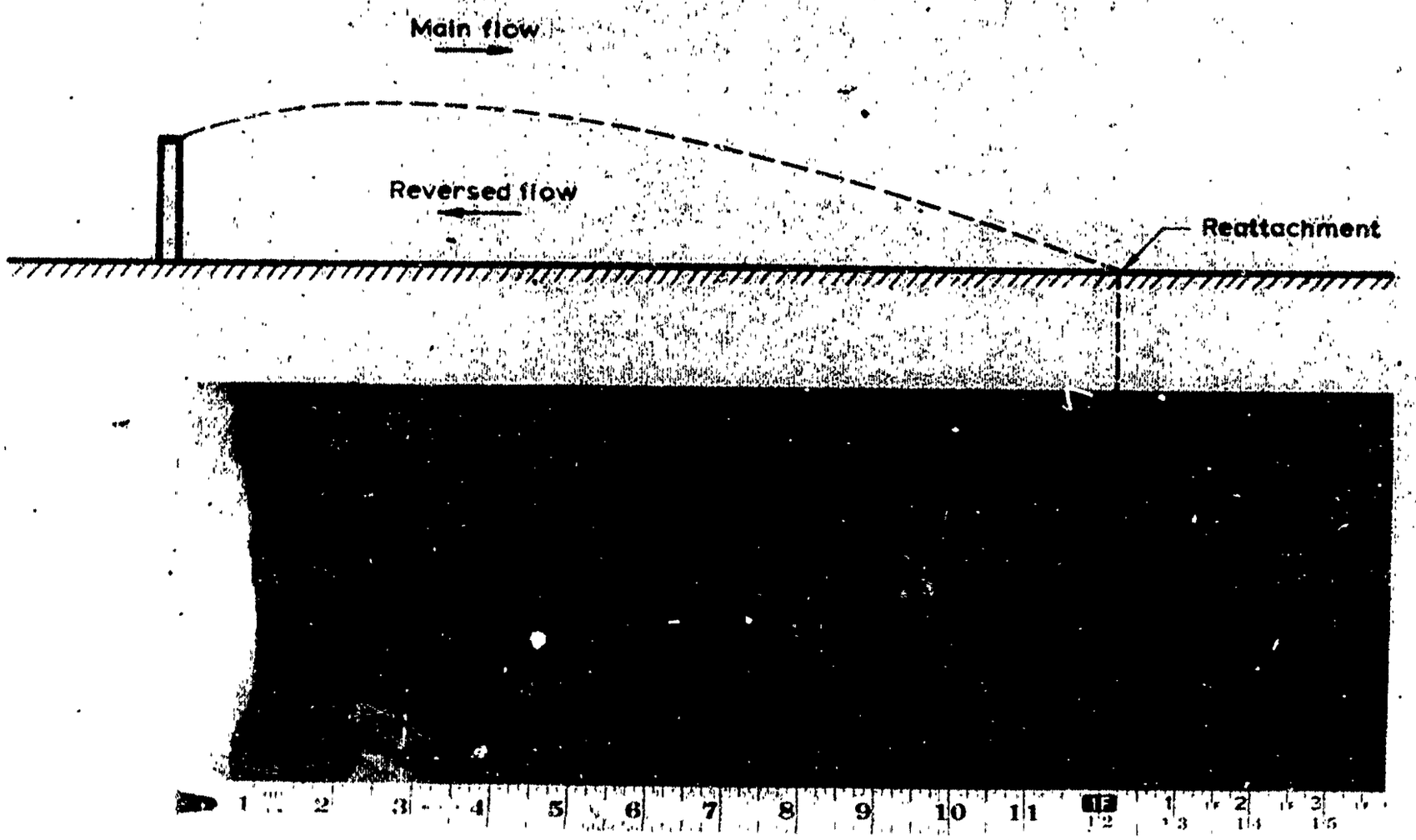
Main flow
Reversed flow
Reattachment

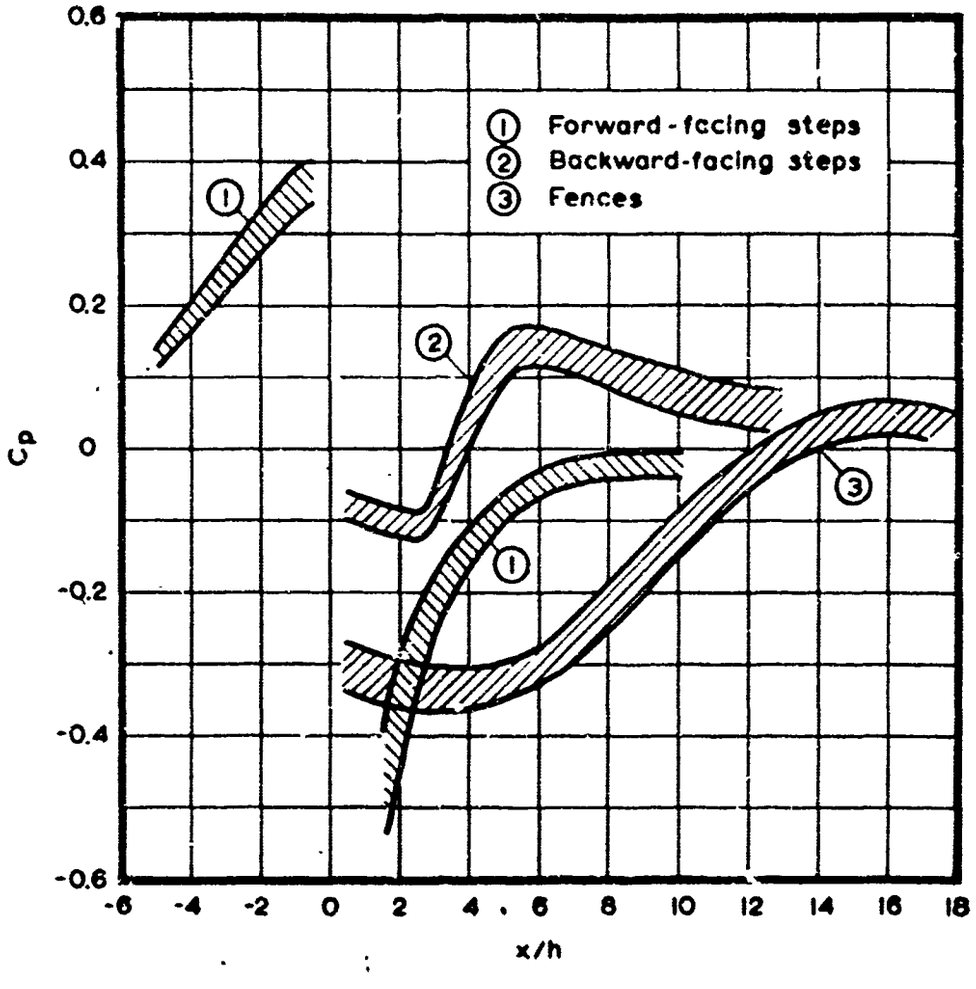
0.6
0.4
0.2
0
-0.2
-0.4
-0.6
C_p
-6
-4
-2
0
2
4
6
8
10
12
14
16
18
x/h
① Forward-facing steps
② Backward-facing steps
③ Fences

AD 1546 D

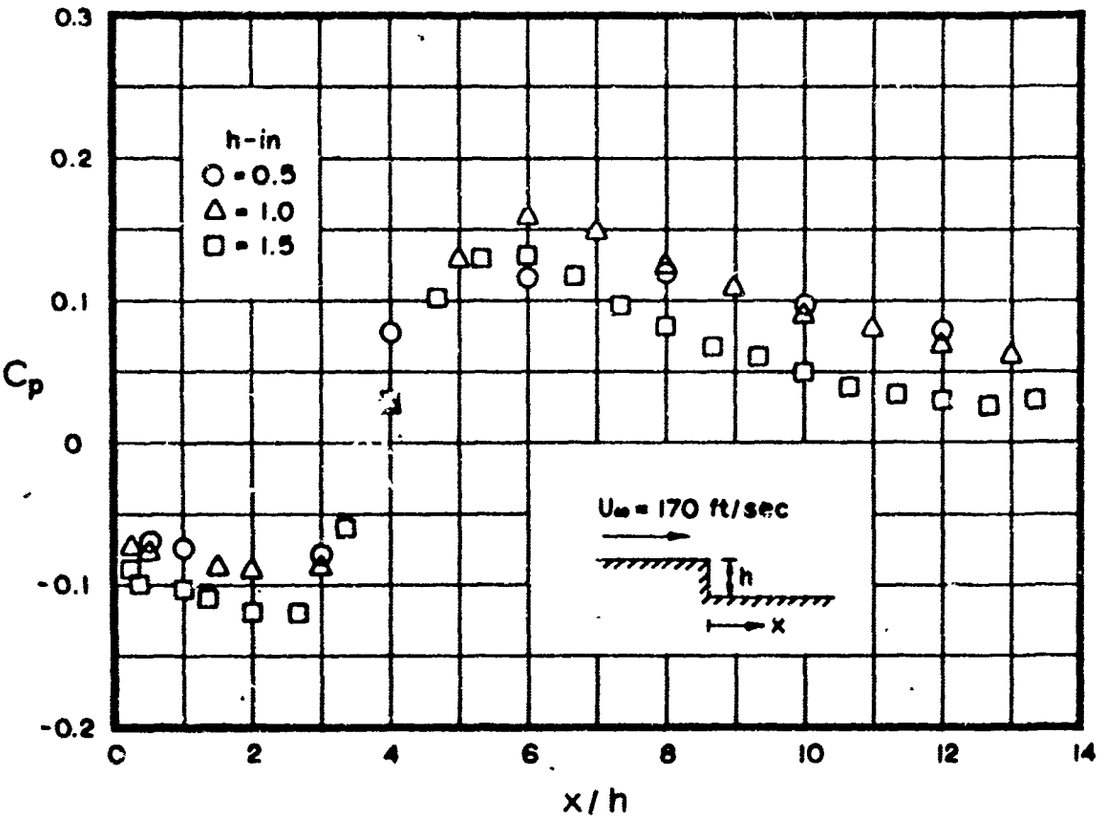

FIGURE 13. PRESSURE COEFFICIENT FOR [illegible] AT 170 FT/SEC.

AC 1546 D

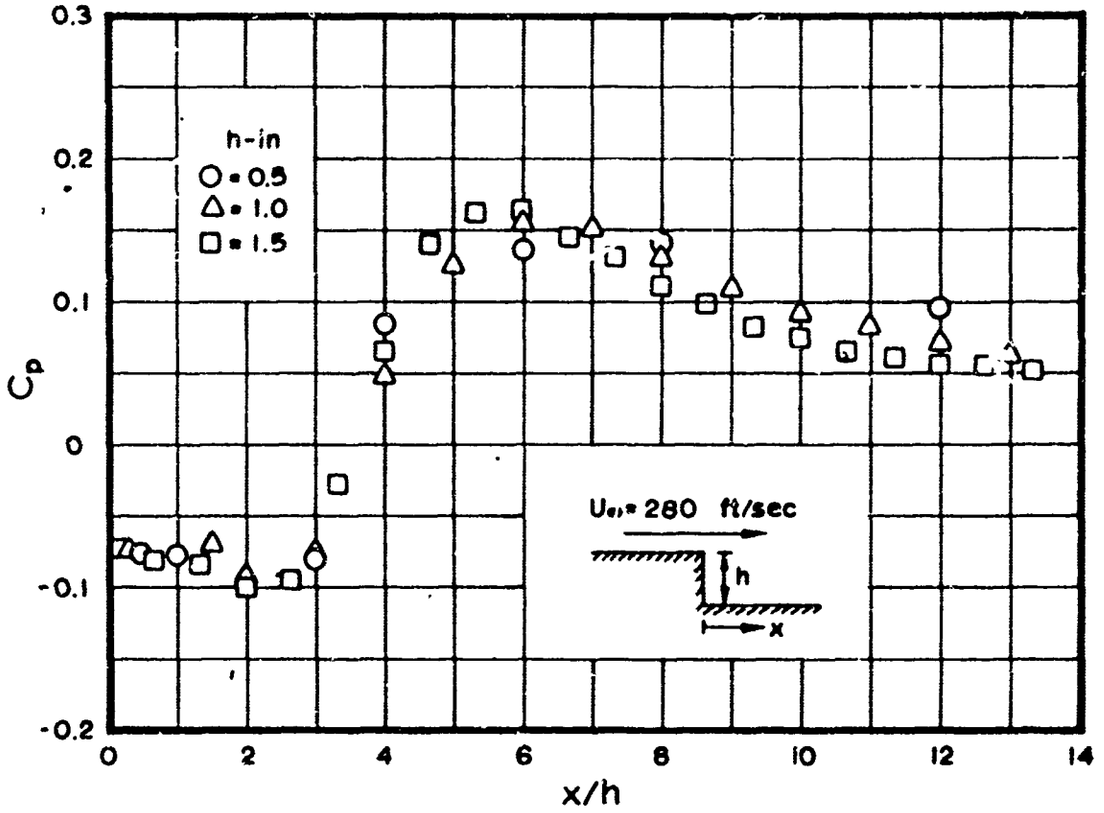
0.3
0.2
0.1
0
-0.1
-0.2
C_p
h-in
○ = 0.5
△ = 1.0
□ = 1.5
U_∞ = 280 ft/sec
h
x
0
2
4
6
8
10
12
14
x/h

AD 1546 D

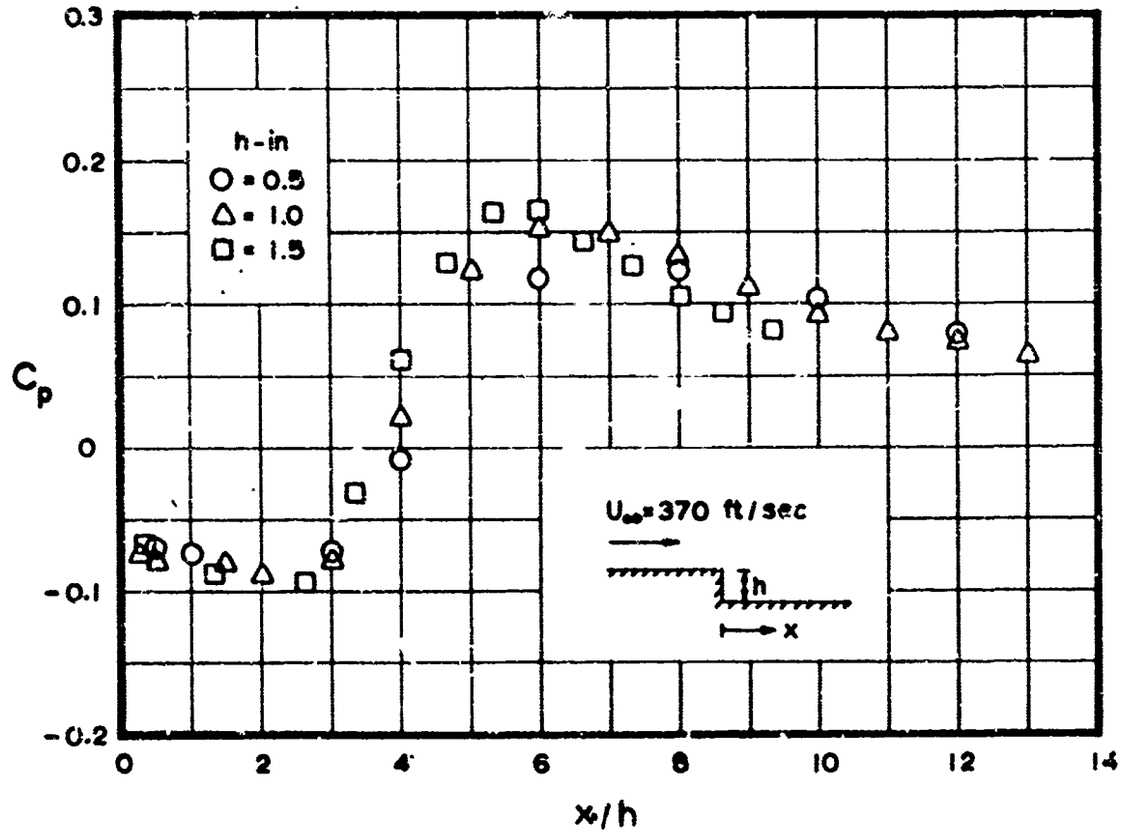

FIG. 15. AR 3506 COEFFICIENT FOR [illegible] AT 370 FT./SEC.

AD 1546 D

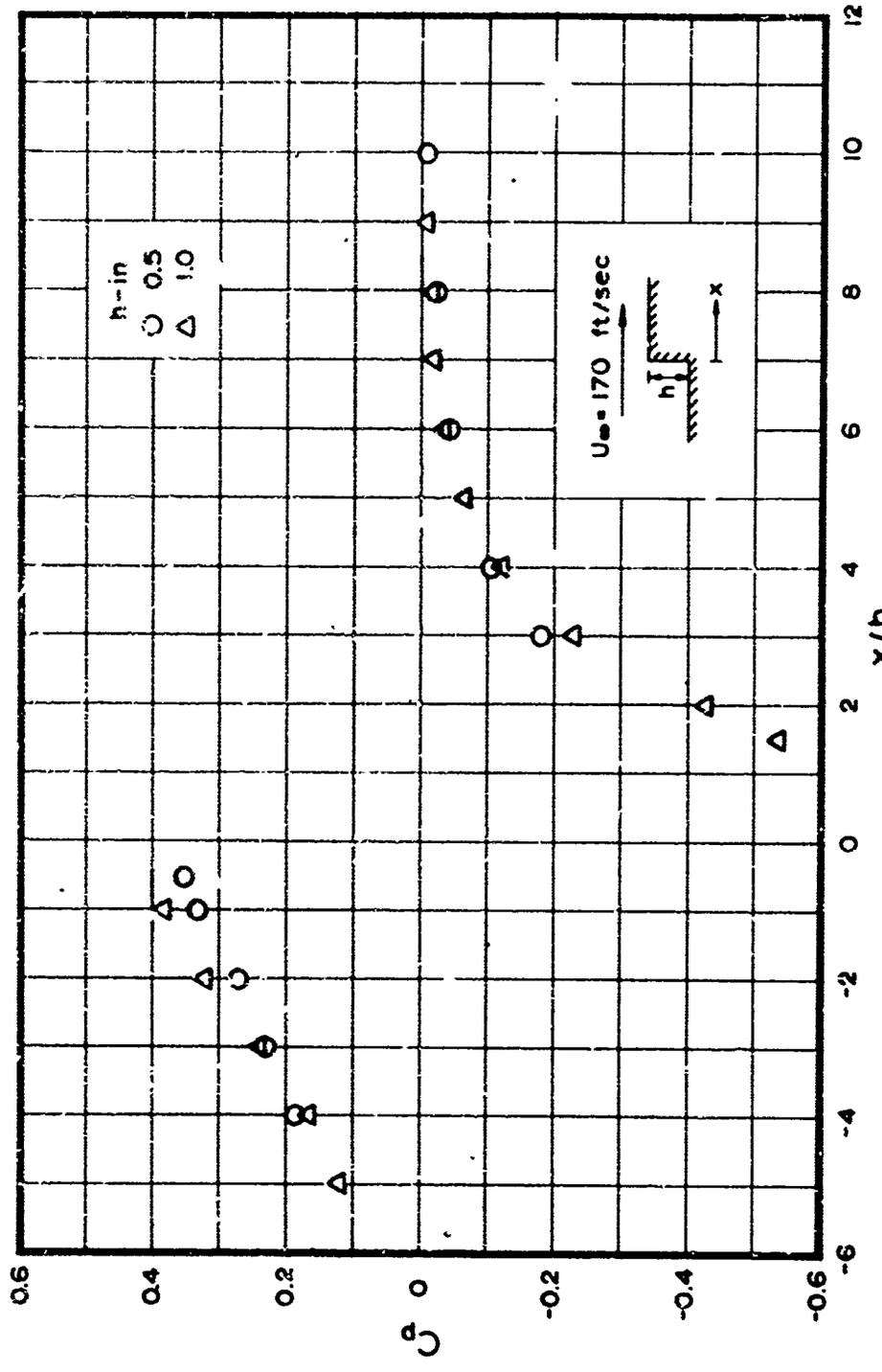

AD 1546 D

REV SYM

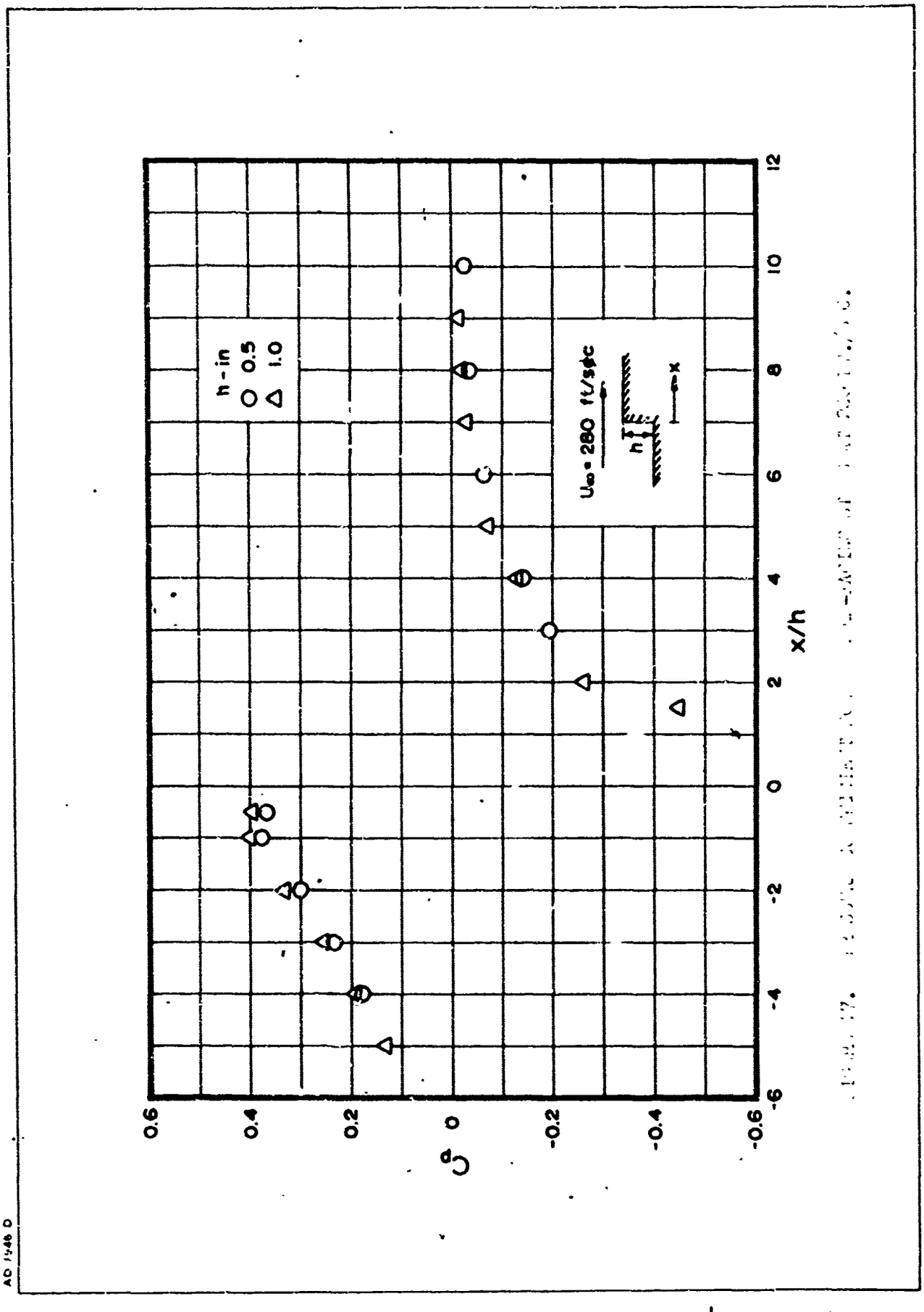

AD 1246 D

REV SYM

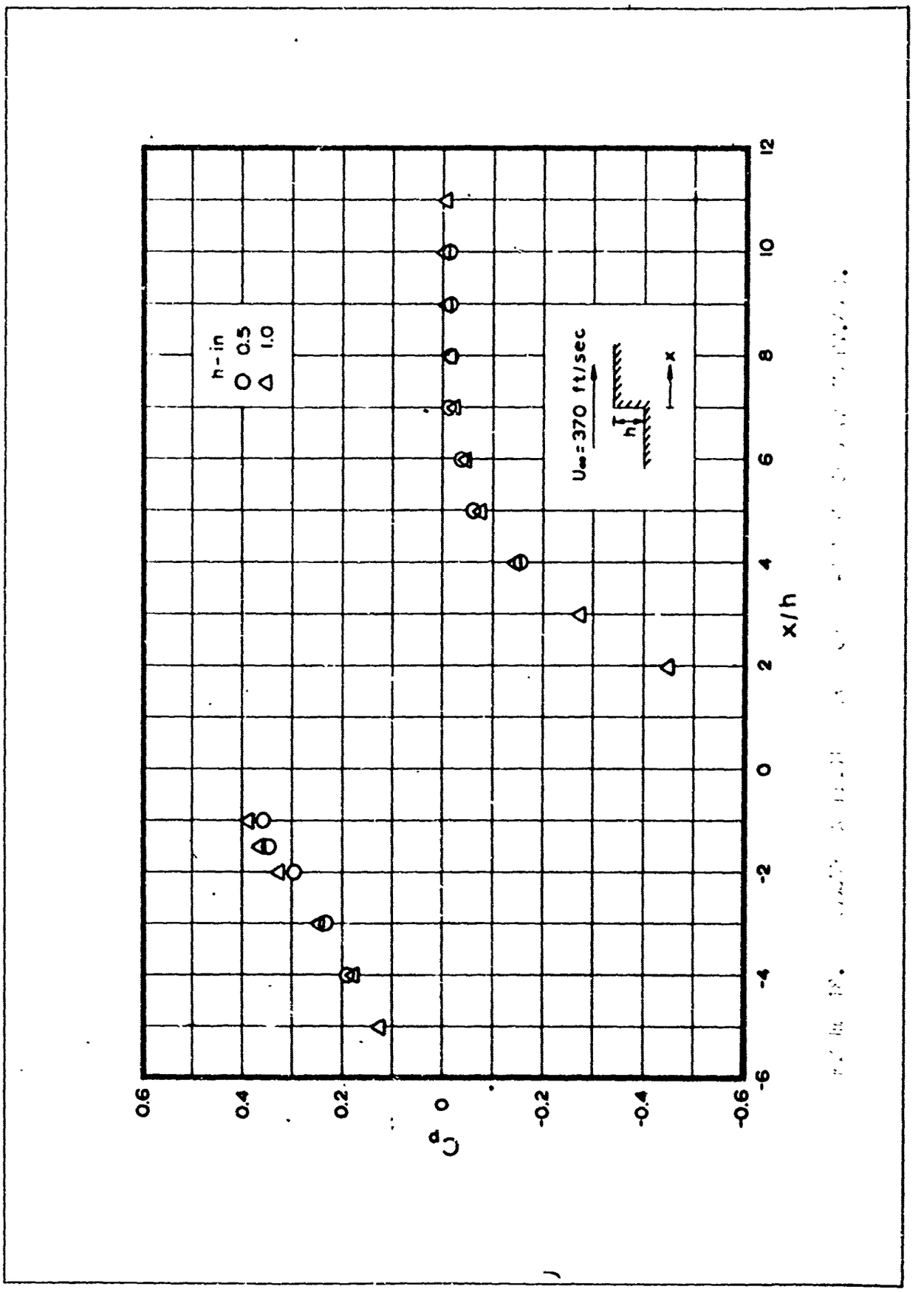

AD 1546 D

REV SYM

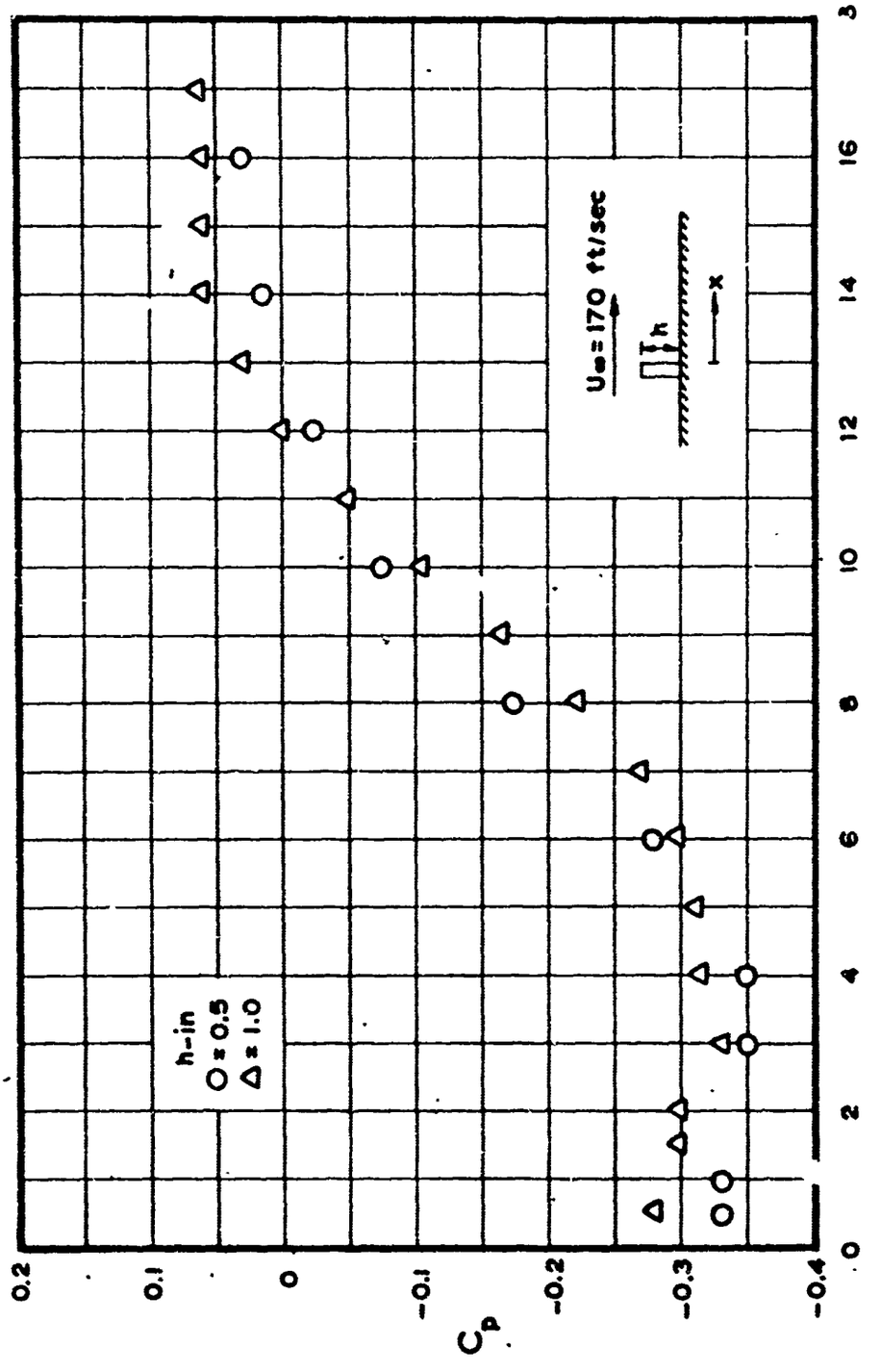

AD 1546 D

REV SYM

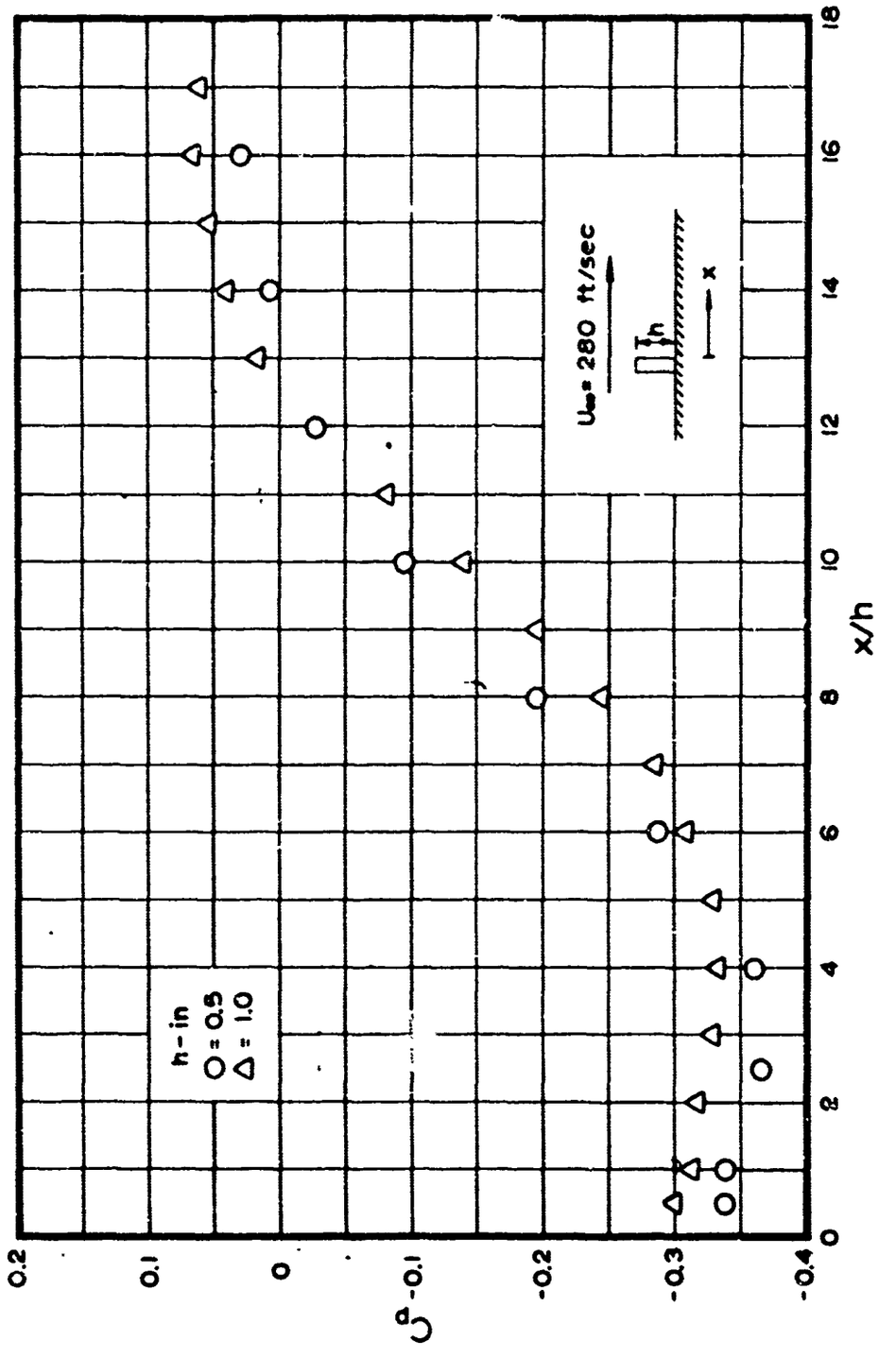

AD 1546 D

REV SYM

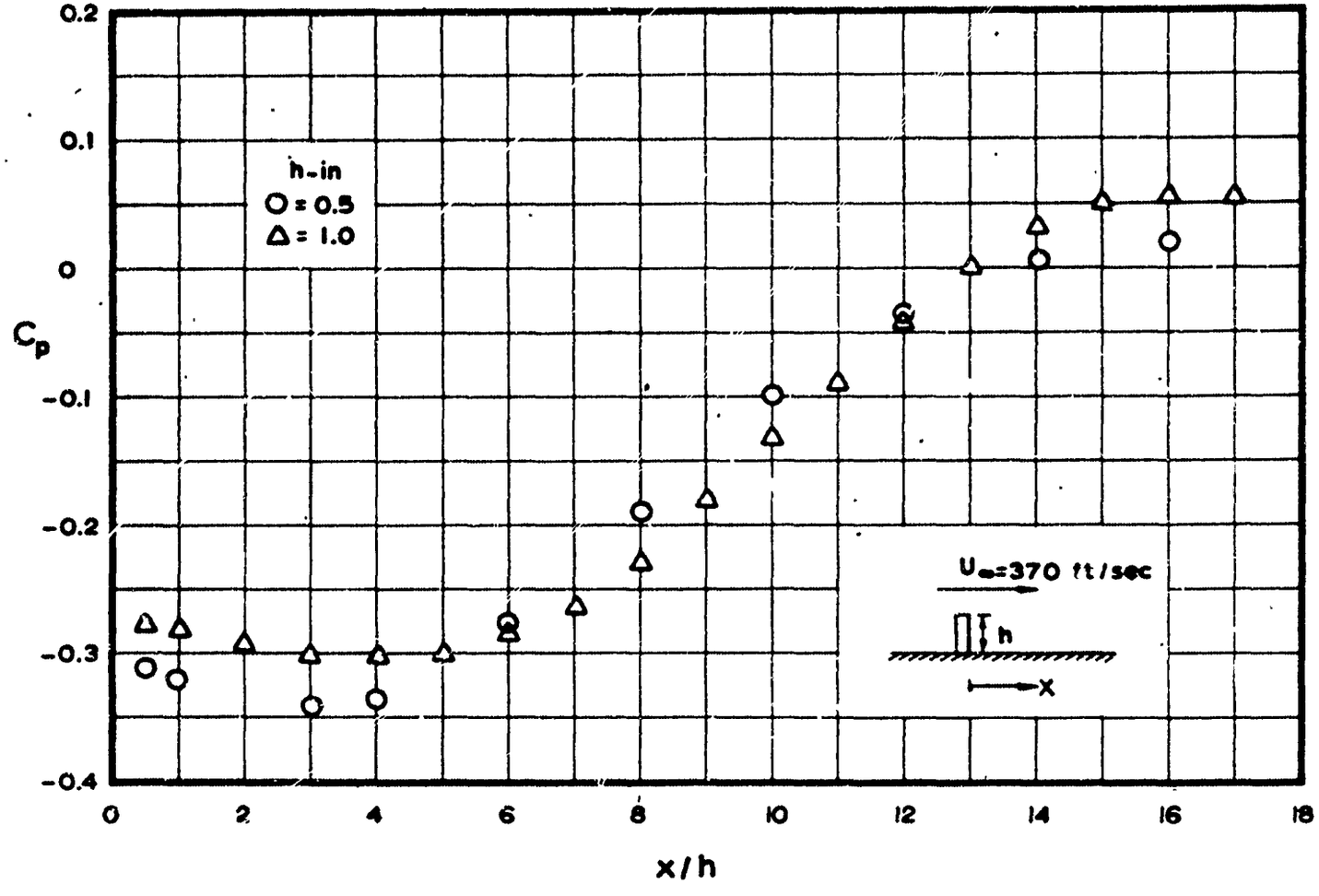

FIGURE 21. [illegible] AT 370 FT./SEC.

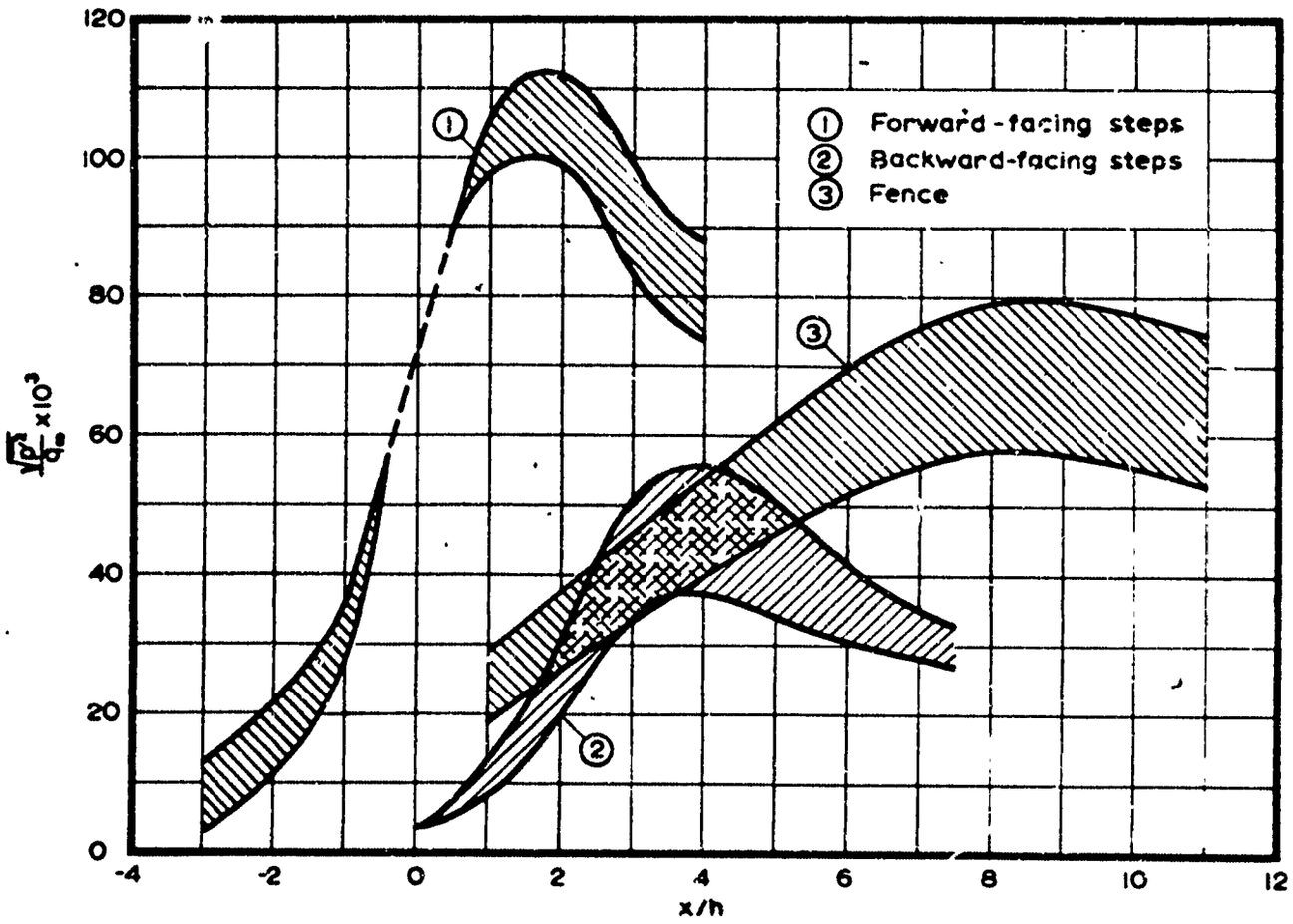

FIGURE 22. BOUNDARY LAYER WALL PRESSURE FLUCTUATIONS FOR [illegible]-FACING STEPS 0.5 IN. 1.0 INCH HIGH, [illegible] STEPS 0.5, 1.0 AND 1.5 INCHES HIGH, AND FENCE 0.5 INCH HIGH FOR ALTITUDES 170,280 AND 370[illegible]

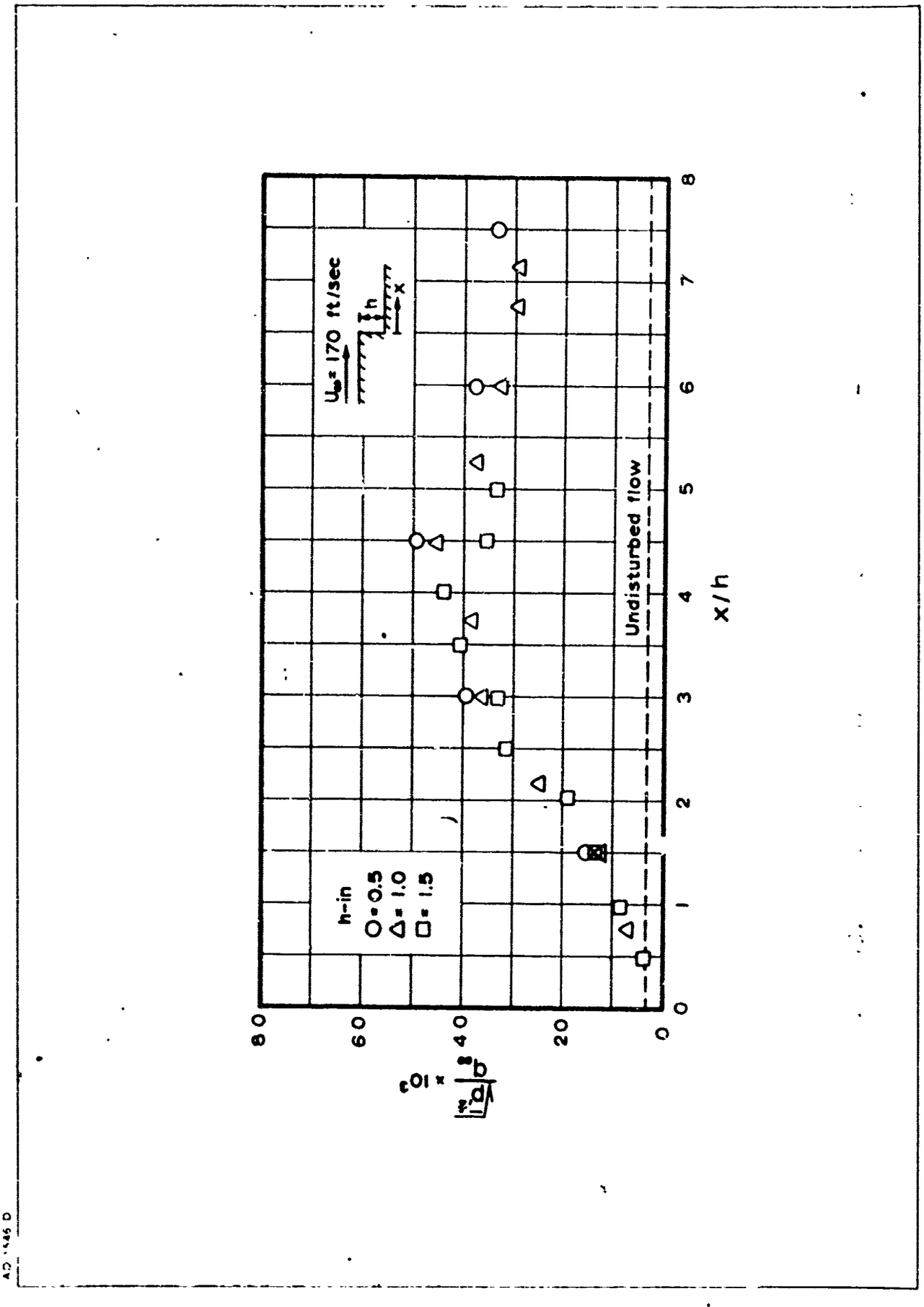

AD 1445 D

REV SYM

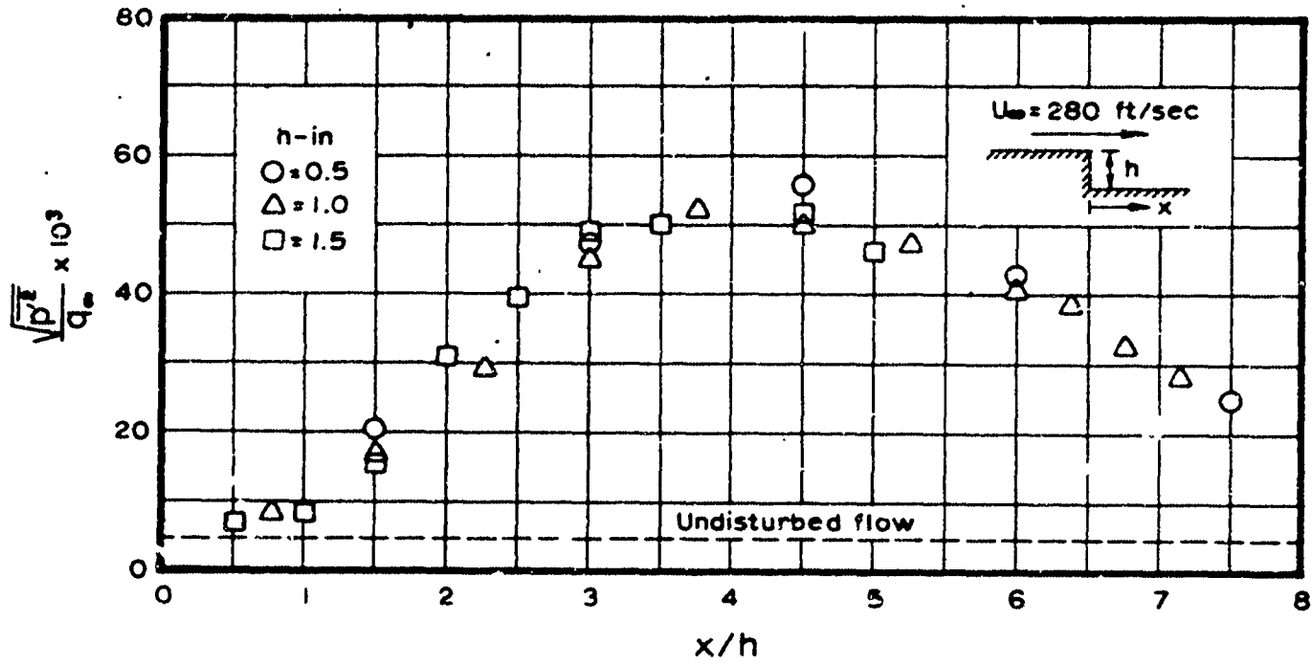

FIGURE 24. FLUCTUATING [illegible] DISTRIBUTION [illegible] 3-PANEL SET AT 280 F./SEC.

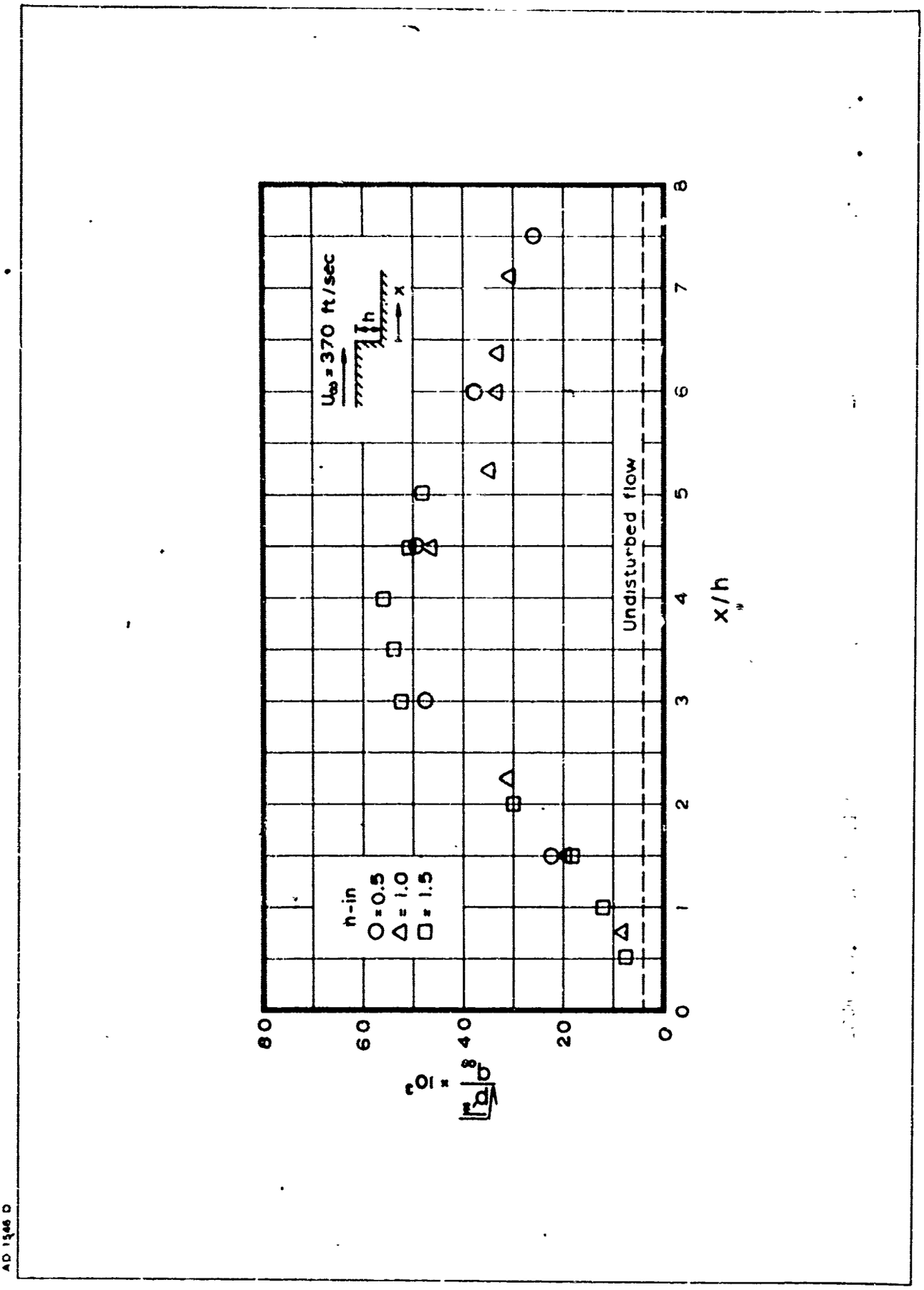

AD 1346 D

REV SYM

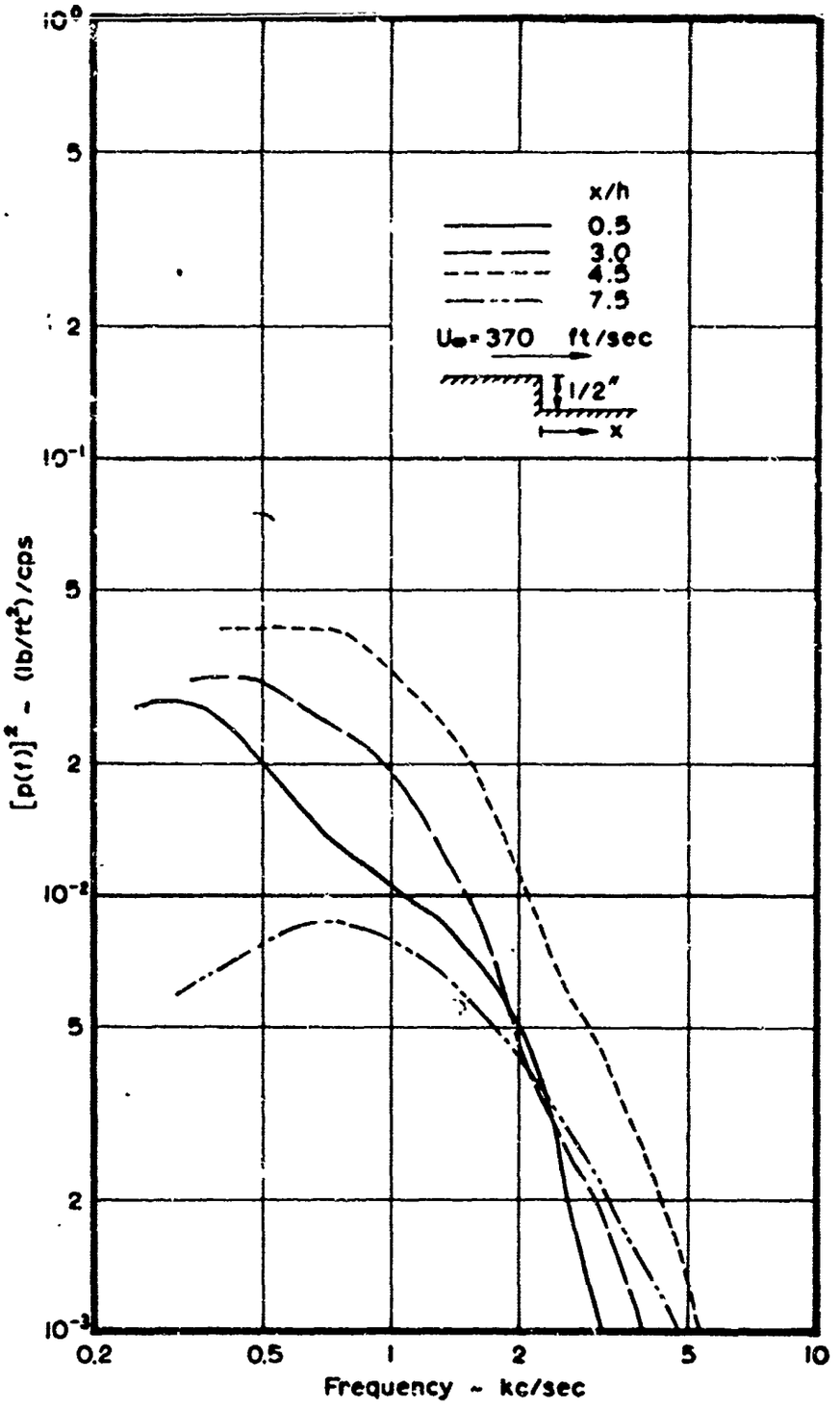
x/h
0.5
3.0
4.5
7.5
U∞ = 370 ft/sec
1/2"
x
[p(f)]² - (lb/ft²)/cps
Frequency - kc/sec
10⁰
5
2
10⁻¹
5
2
10⁻²
5
2
10⁻³
0.2
0.5
1
2
5
10

FIGURE 26. [illegible]

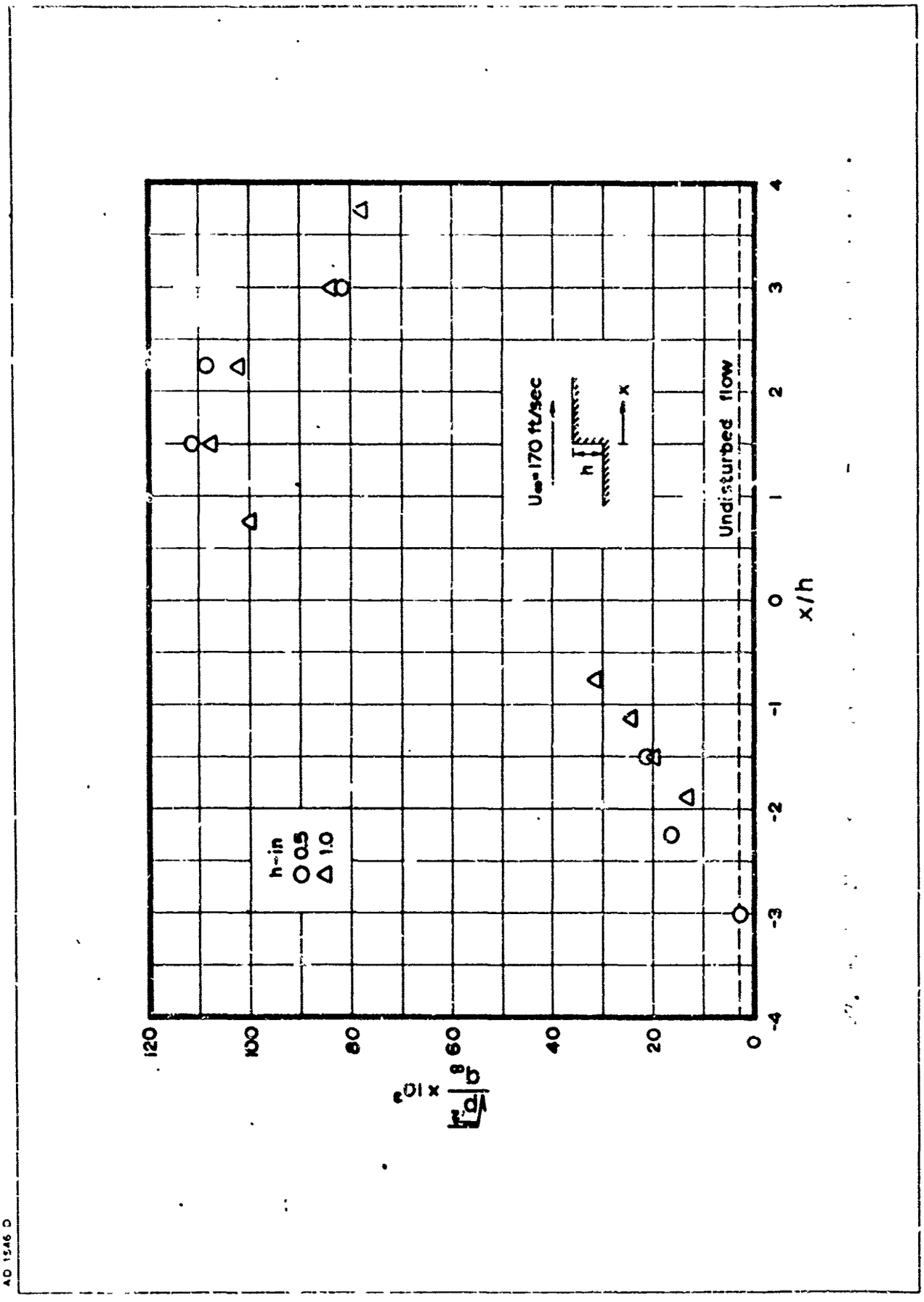

AD 1546 D

REV SYM

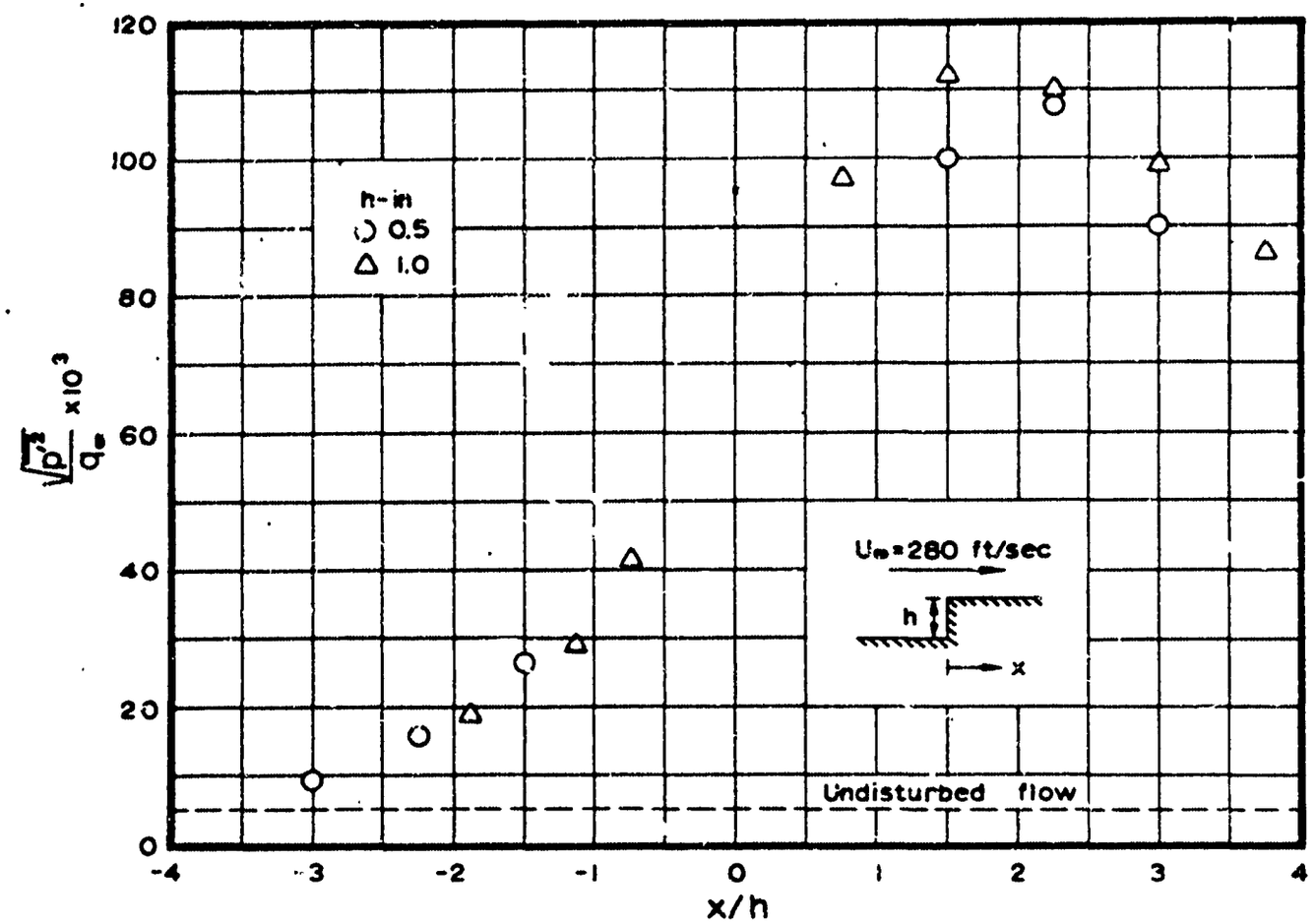

FIGURE 28. [illegible] AT 280 FT./SEC.

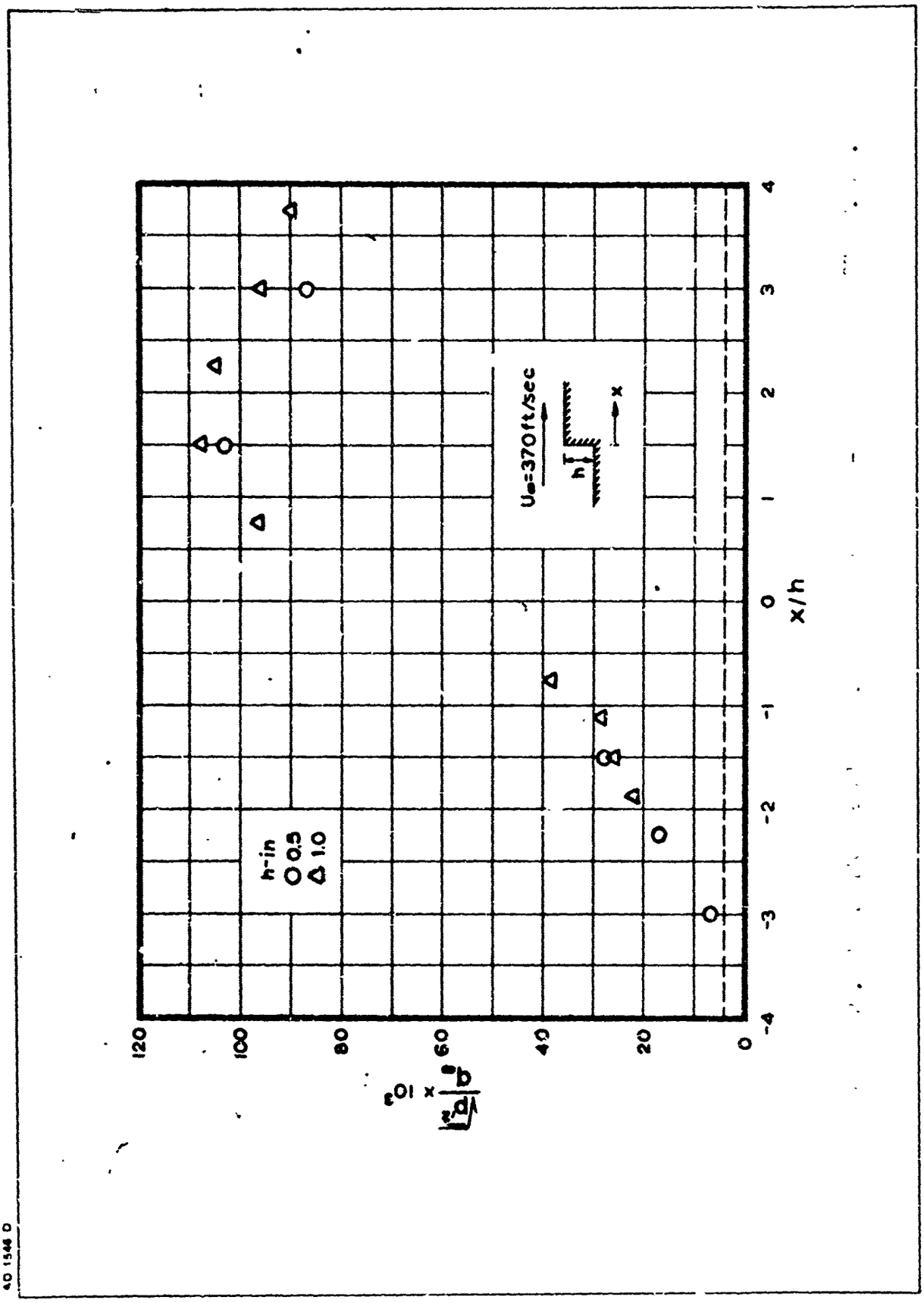

40 1544 D

REV SYM

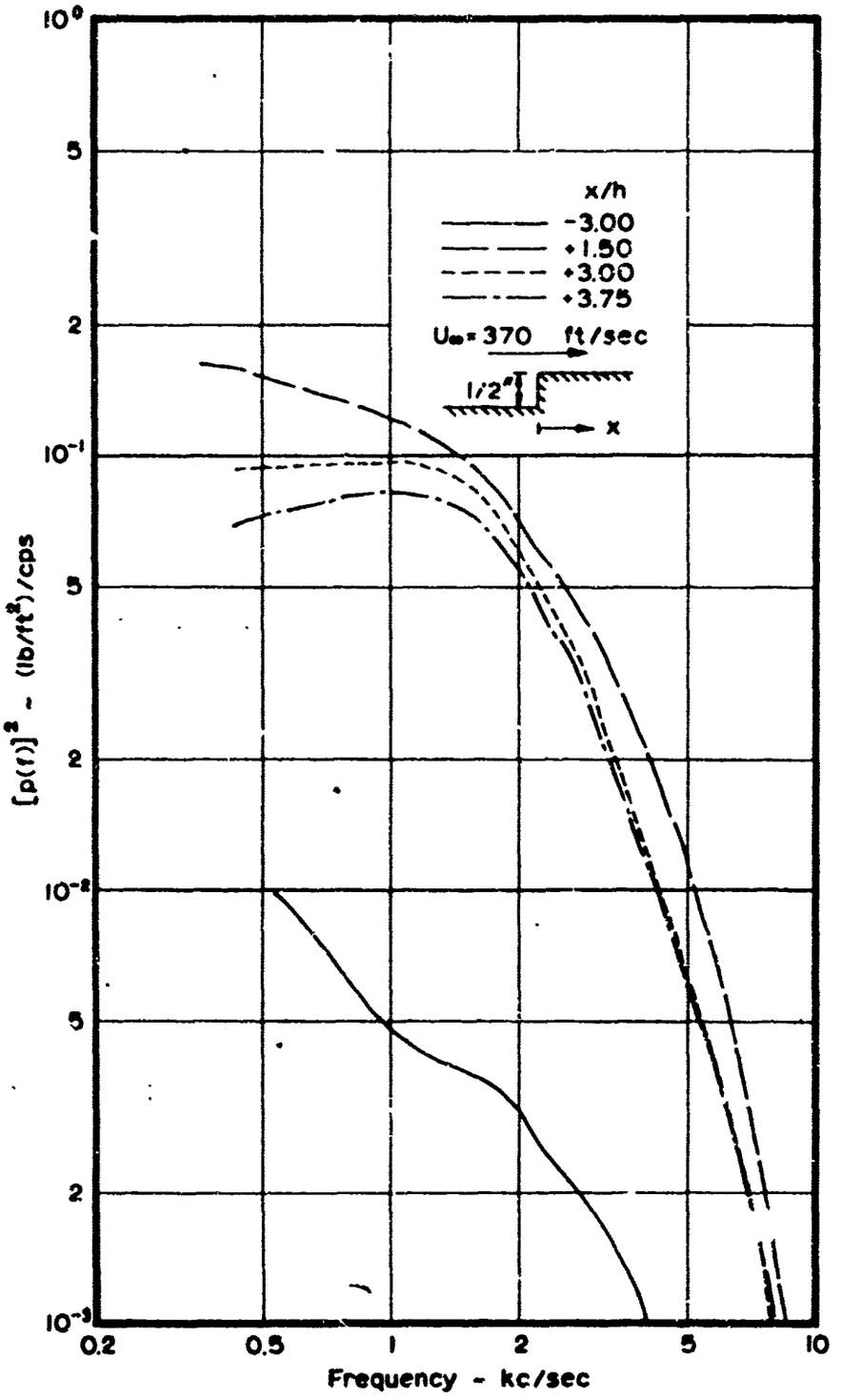

FIGURE 30. [illegible] U∞ = 370 FT./SEC.

AD 1546 D

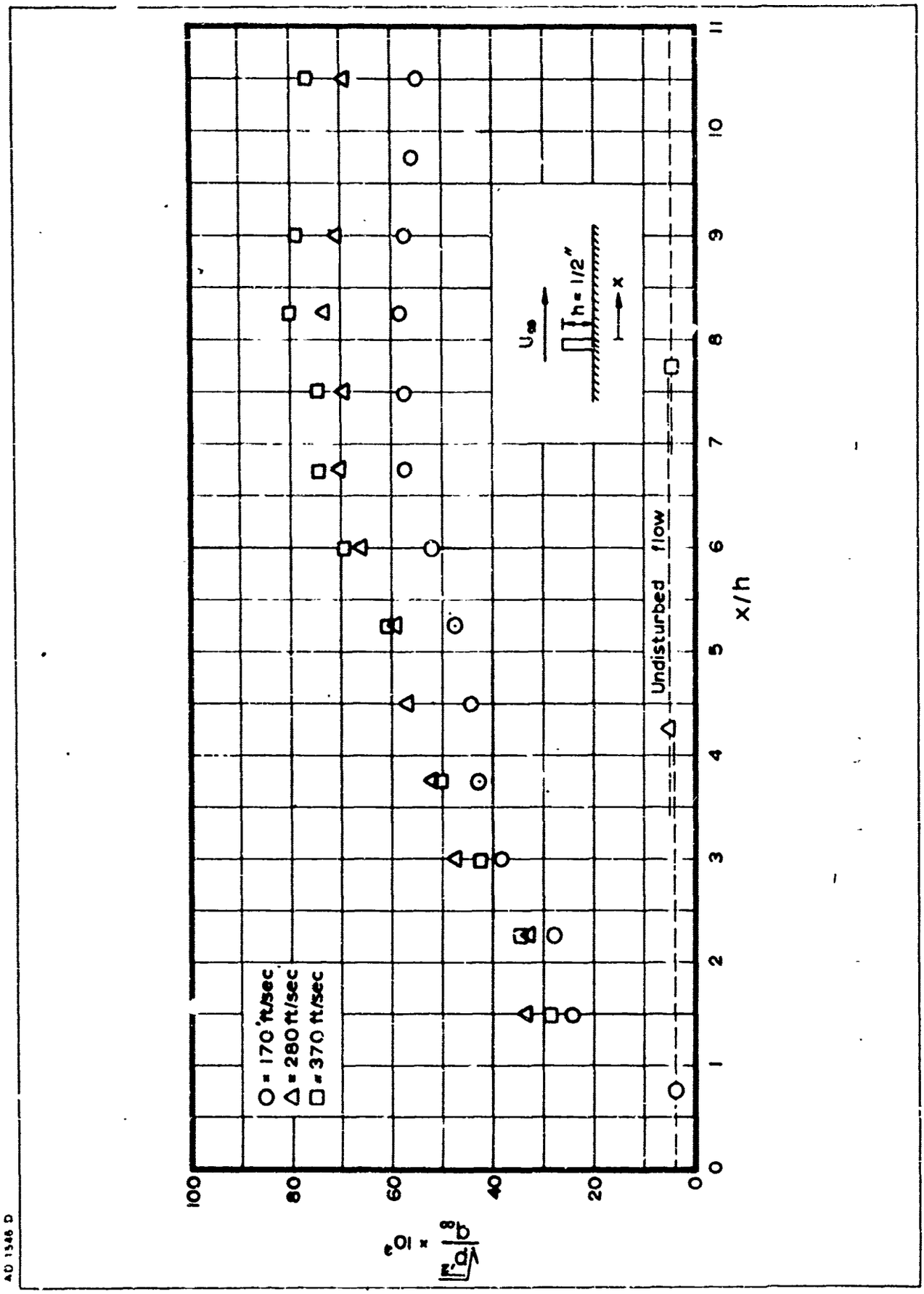

AD 1348 D

REV SYM

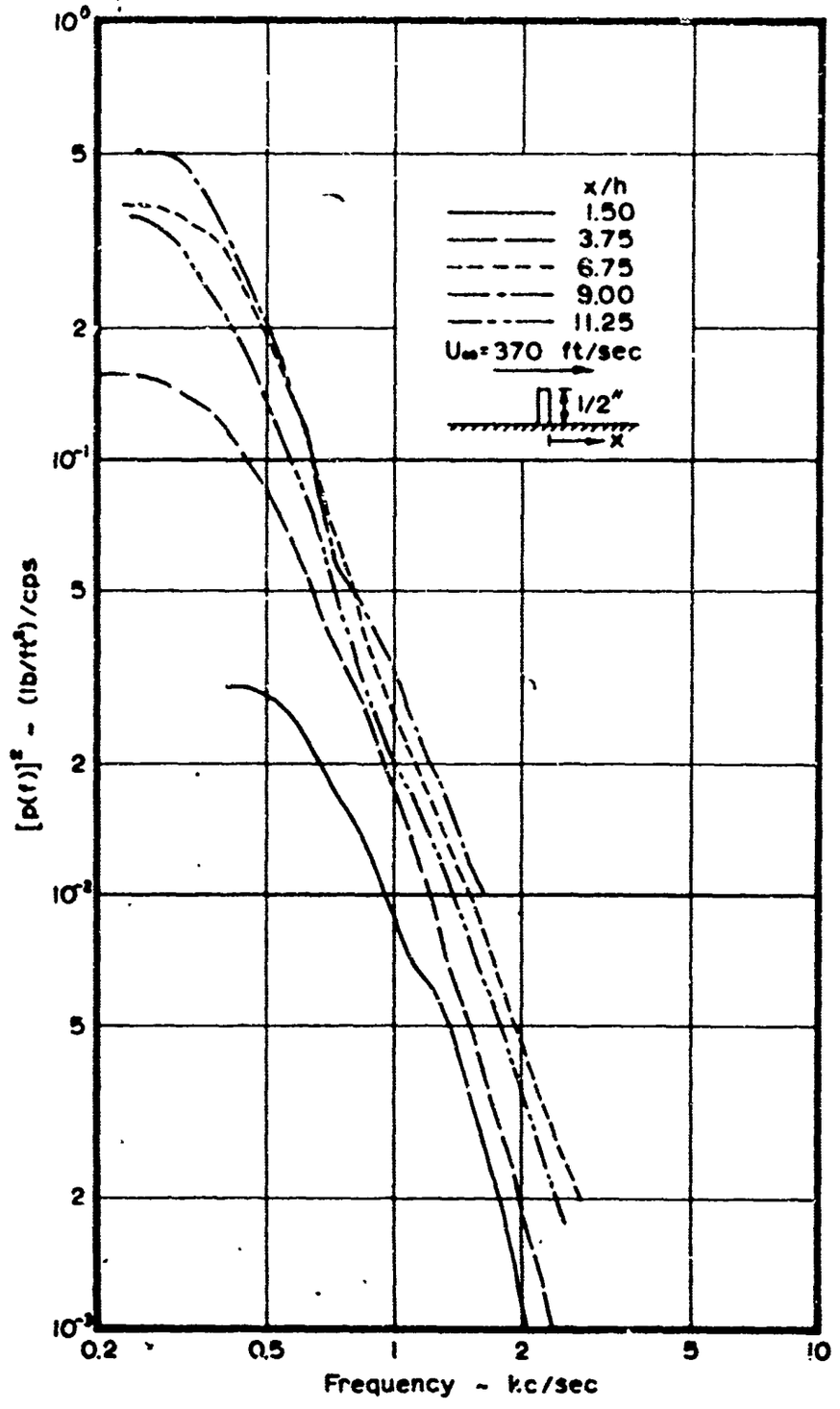

FIGURE 32. POWER SPECTRAL DENSITY FUNCTIONS AT 370 FT./SEC.

AD 1546 D

APPENDIX

Description of Apparatus

Air Supply

The air flow was supplied from the exit plane of the Boeing Subsonic Boundary Layer Facility sketched in Figure A1. The facility is an open circuit continuous flow air tunnel consisting of 24 feet of rectangular duct having maximum mass flow rate of 0.26 slugs/sec and maximum Mach number of 0.85. Prior to the exit plane of the facility, the flow becomes fully turbulent pipe flow with an effective boundary layer thickness equal to 2.0 inches.

Test Section

Details of the experimental arrangement used in the present investigation are shown in Figures A2 and A3. The test section consisted of two rectangular U-shaped aluminum open channels. The upstream channel (7" wide, 6" high, and 18" long) was fastened with its interior surfaces flush with those of the exit plane of the duct facility. The downstream channel (7" wide, 8" high, and 32" long) was mounted on a hydraulic jack so that its floor could be lowered or raised, with respect to that of the upstream channel, to generate backward- or forward-facing steps respectively. Also, with the channel floors positioned at the same level, fences could be inserted and fastened along the line formed by the junction of the two channels. The U-shaped rectangular test section was selected in order to obtain a region of two-dimensional flow at the centerline of the test section.

Static Pressure Measurements

Static pressure ports, spaced 1" apart, were drilled along the centerline of the test section and were spaced 1" apart starting 1" from the exit plane of the air supply. The pressures from the different ports were recorded individually on water manometers.

Total and Static Pressure in the Flow

The motor driven mechanism shown in Figure A4 was used to traverse the flow in the vertical plane containing the centerline of the test section. The total and static pressures in the flow were measured separately by fitting the appropriate probe to the traverse mechanism. The output of the probe was fed to a Statham gauge which was connected to an x-y plotter. In the region of flow reversal, two total pressure traverses were taken; one full traverse with the total pressure probe facing upstream, and another traverse with the probe facing downstream to a height slightly greater than that of the geometry causing flow separation.

Wall Pressure Fluctuations

A separate downstream channel, identical in dimensions to the one used for the aerodynamic measurements, was made for the measurement of the wall pressure fluctuations. In that channel, 1/4-inch diameter holes were spaced 3/8-inch apart starting at 3/8-inch from the upstream edge of the channel. These holes were used to insert flush 1/4-inch B & K microphones, the output of which was fed through the circuit shown in Figures A5 to an FM tape recorder. Spring loaded plugs were used to plug the holes in which no measurements were being taken.

Hot Wire Measurements

Measurements of the mean and fluctuating velocity components, U and u', were made in the undisturbed flow upstream and in the regions of separation and reattachment downstream of a fence using standard hot wire techniques. The instrument used was a Model 1956 Aeroresearch constant temperature hot wire anemometer. The probe used for these measurements, illustrated in Figure A6, was mounted on the manually operated traverse mechanism shown in Figure A7. The probe carrying mechanism could be positioned at any streamwise location and retracted away from the bottom surface of the test section.

Flow Visualization

Two visual techniques were employed to assist in the interpretation and reduction of the flow measurement data.

The first technique, used to study the flow pattern on the floor of the test section, in the regions of flow reversal and reattachment, consisted of spreading a thin layer of a solution of lampblack dissolved in paint thinner. Photographs of the lampblack deposit, shown in this report were then taken.

The second technique was evolved for the purpose of locating the zero-velocity line. The probe illustrated in Figure A6 was developed for this purpose, and was used as a wind-vane in the flow. The vane was made out of steel shim 0.01 inch thick soldered to one end of a 1/32 inch diameter steel wire which acted as a shaft inside the stainless steel sleeve. Brass weights were used to increase the inertia of the vane with the larger one used when the flow fluctuations were too intense. The conical tip of the brass weight pivoted on a piece of Teflon placed inside the body of the probe. A few drops of oil were added to lubricate the movement of the steel shaft and to dampen the high amplitude fluctuations of the vane.

The traverse mechanism shown in Figure A7 was used to vary the height of the zero-velocity probe above the floor of the duct. As the probe traversed the zero-velocity region a change in the direction of the vane was observed. An average of the change-over heights for two opposite traversing directions was then taken as a point on the zero-velocity line.

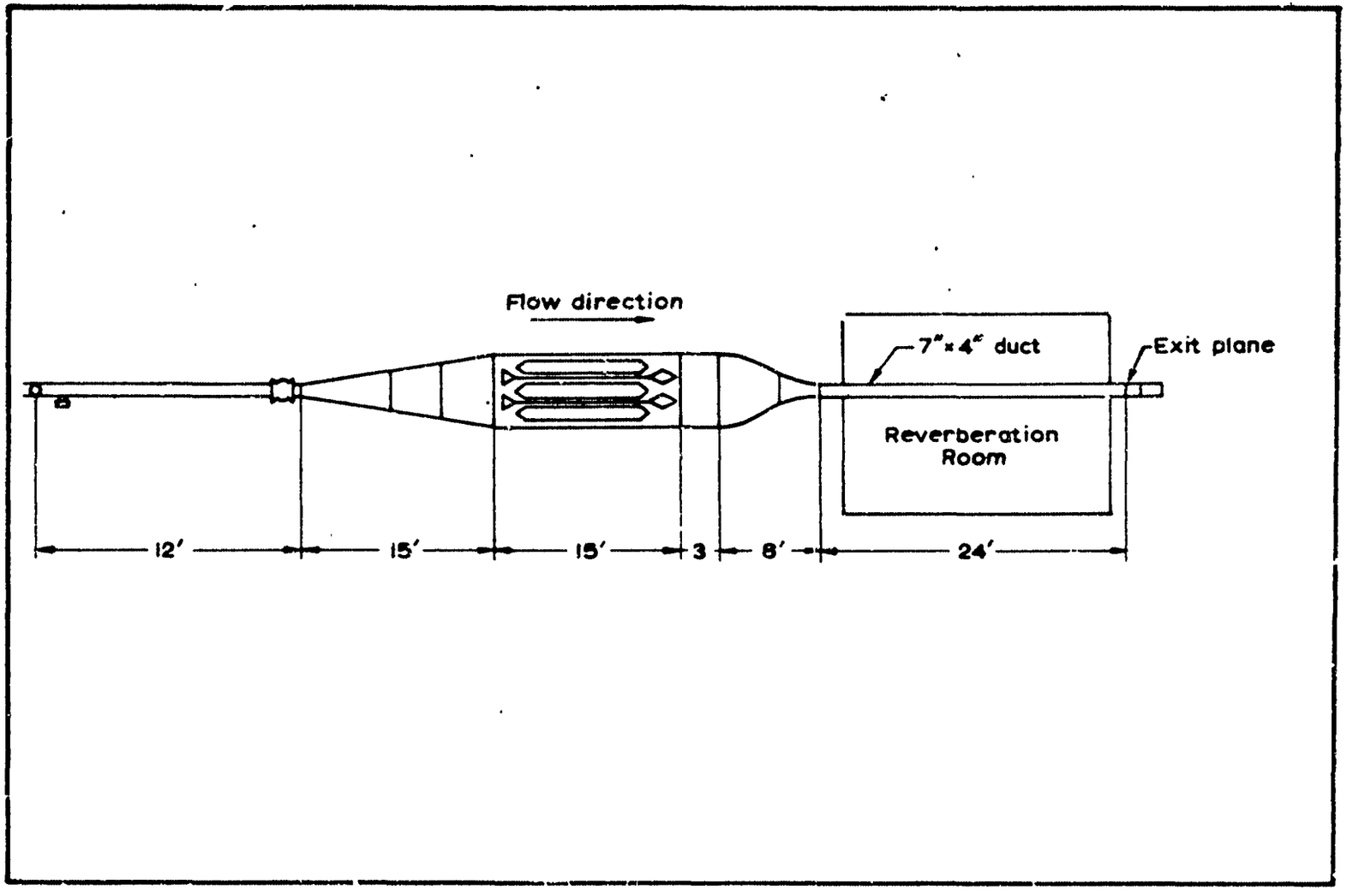
Flow direction
7" × 4" duct
Exit plane
Reverberation Room
12'
15'
15'
3
8'
24'

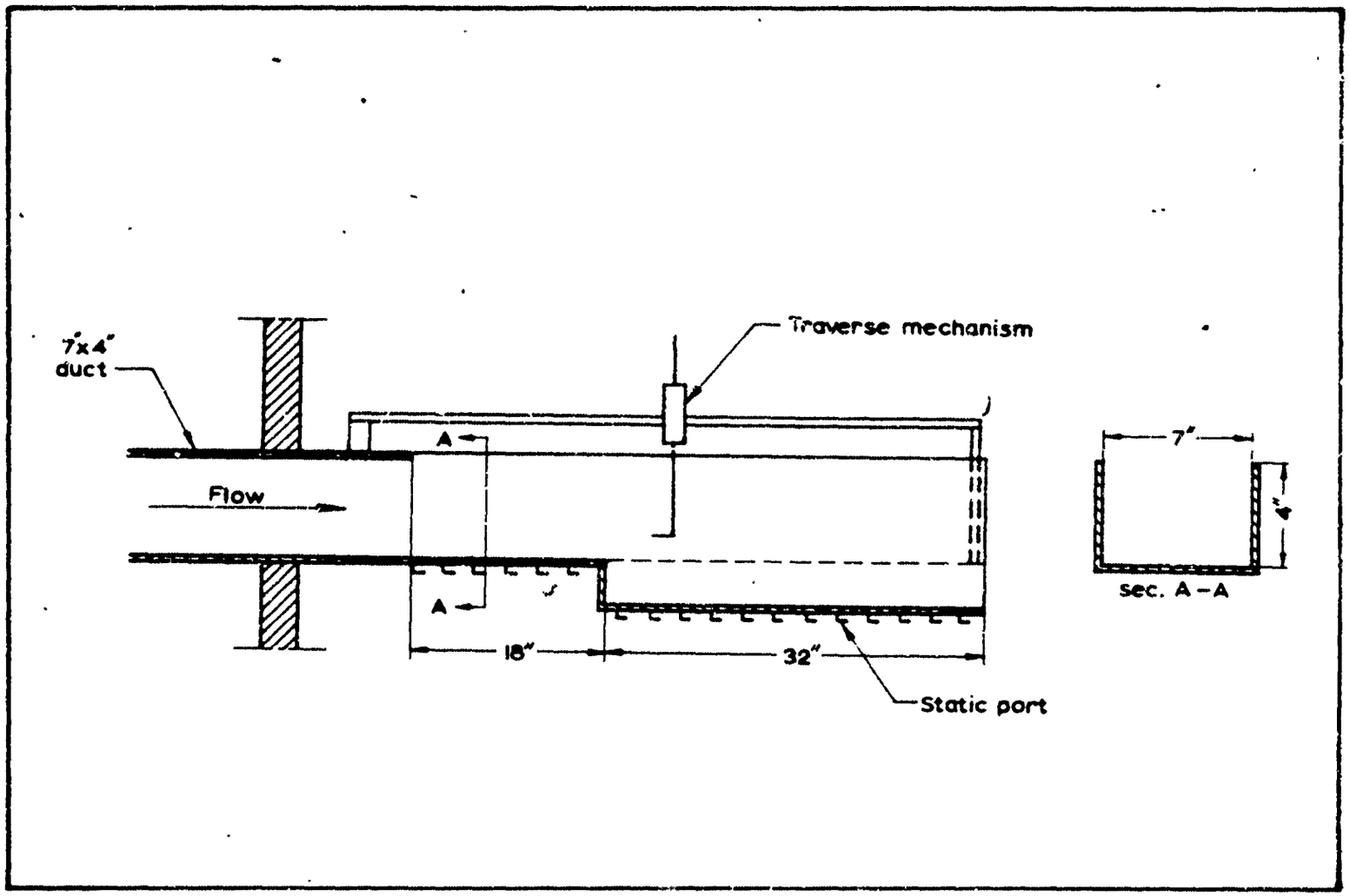

FIG. 6. A.2 LONGITUDINAL CROSS-SECTION OF T-12 SECTION

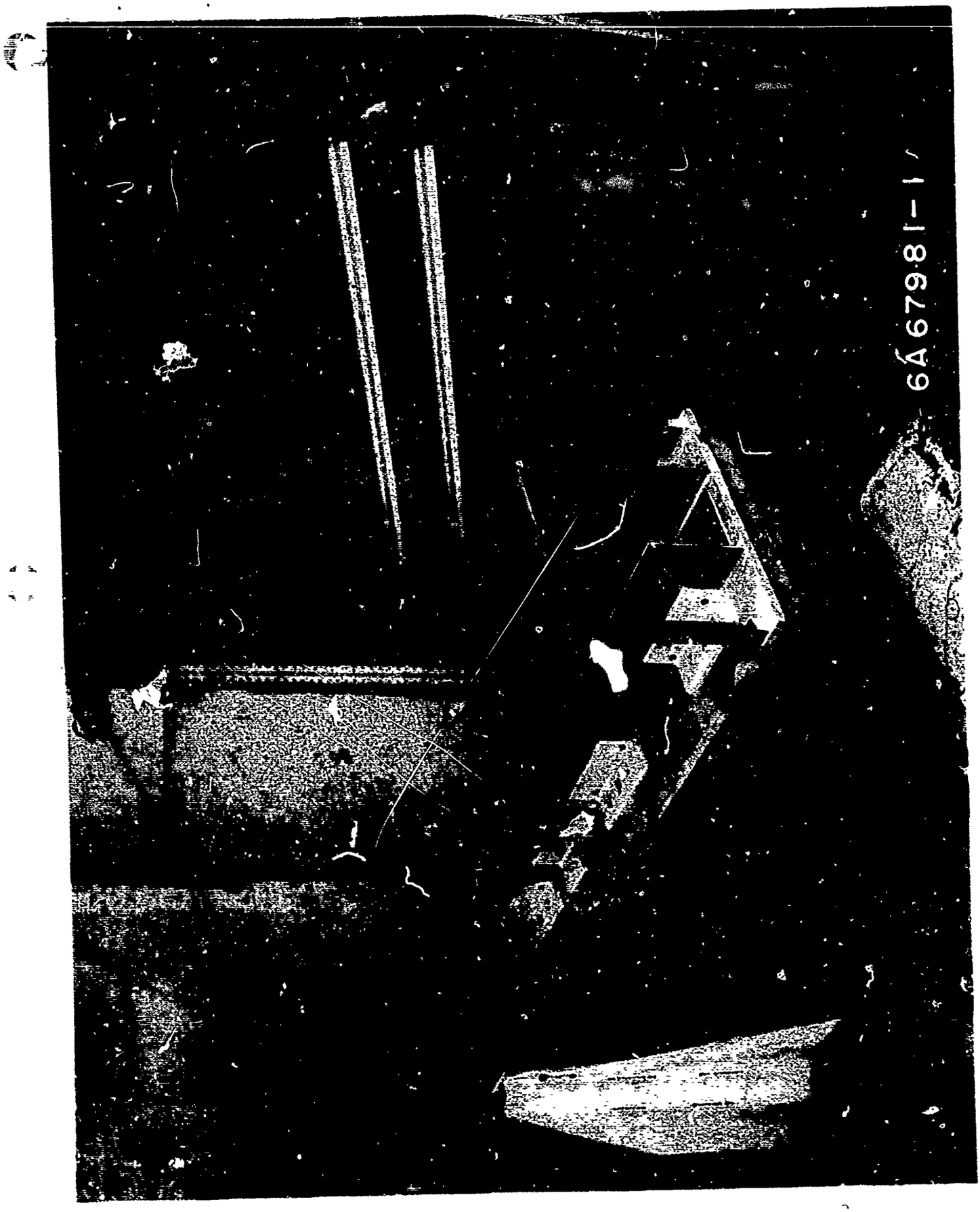

FIGURE A.3 TEST SECTION FOR STUDY OF SEPARATED FLOW.

FIGURE A4. MOTOR-DRIVEN TRAVERSE MECHANISM WITH TOTAL PRESSURE PROBE ADAPTED

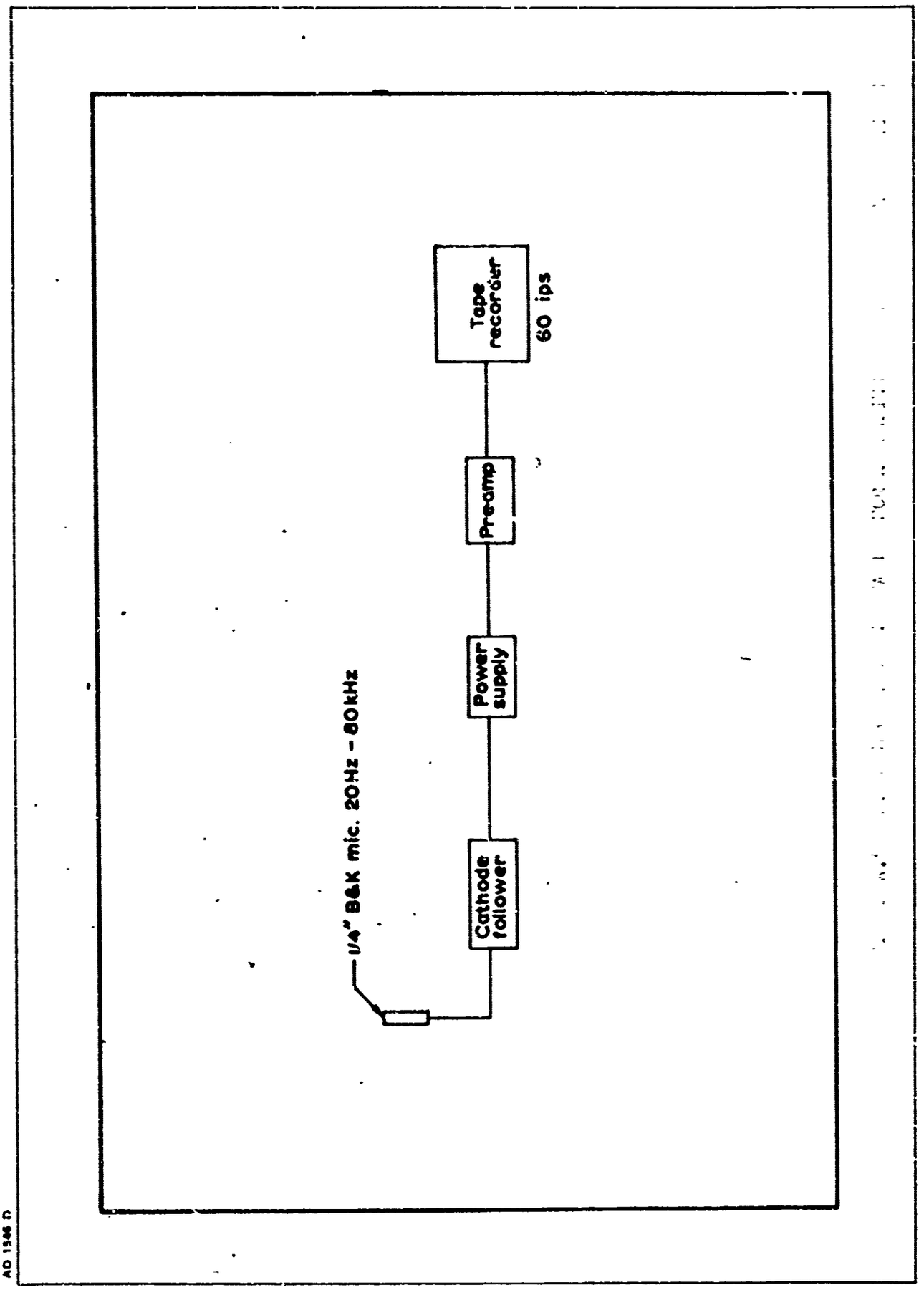

AD 1546 D

REV SYM

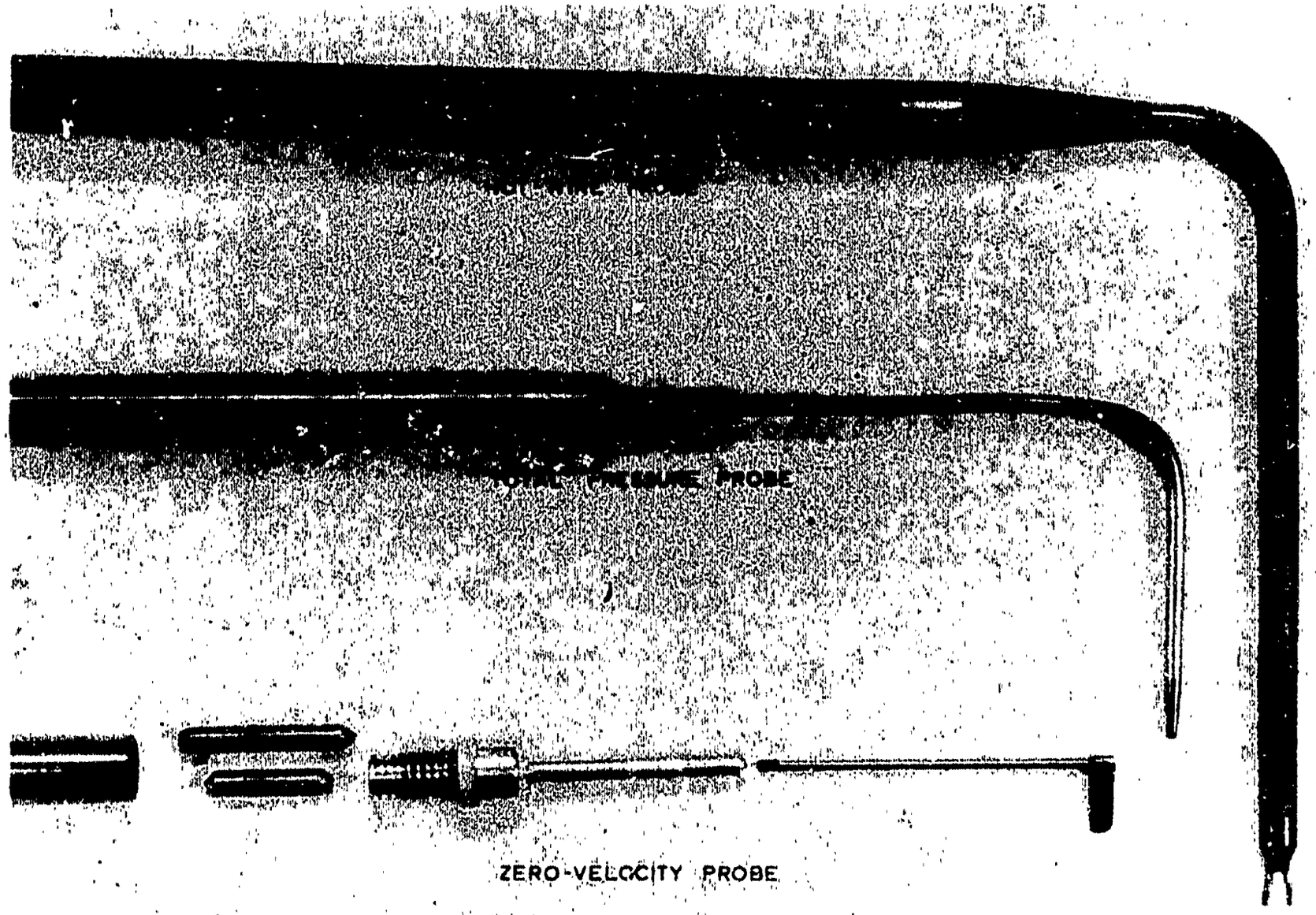

FIGURE A6 VARIOUS MEASURING PROBES

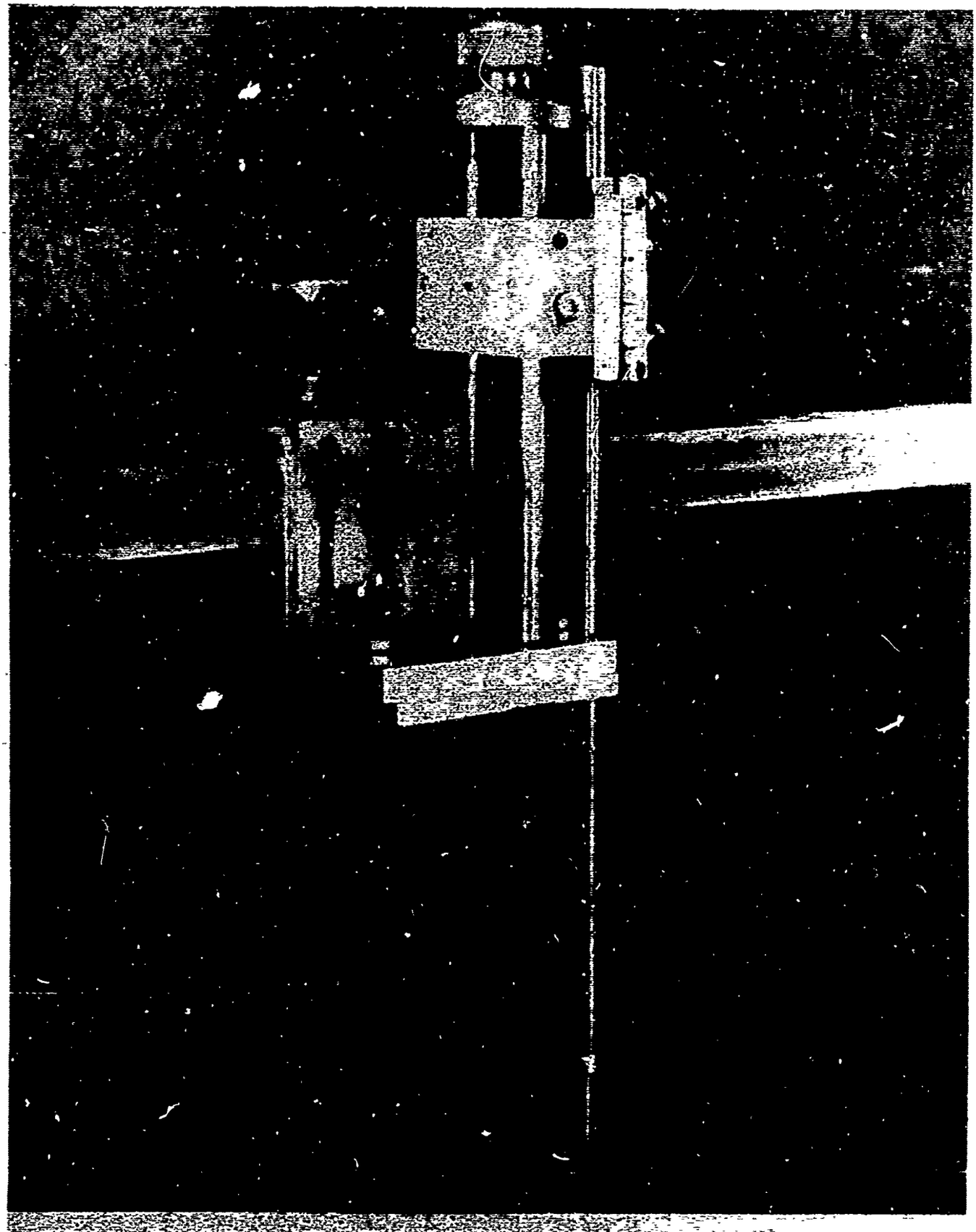

FIGURE A7 MANUALLY [illegible] MECHANISM WITH ZERO-VELOCITY PROBE ADAPTED